REQUEST FOR TESTING SIGNAL AMPLIFICATION OF A NEW LIQUID XENON DETECTOR WITH HIGH BACKGROUND REJECTION IN ORDER TO STUDY GALACTIC DARK MATTER

M Atac, D B Cline, P Picchi[1], Y Seo, F Sergiampietri, and H Wang*

University of California, Los Angeles, California 90095

[1]ICGF-CNR, Corso Fiume 4, Torino, Italy

ABSTRACT

A strong theoretical candidate for WIMP particle is neutralino, the lightest supersymmetric particle (LSP), from the supersymmetry (SUSY) theory, which would be formed in the early universe and subsequently cluster in Galaxies with normal matter. Since no experiments could observe the estimated low event rates, there are intensive world efforts to reach the level of sensitivity enough to measure these neutralino signals from our Galaxy. ZEPLIN II detector which has the best possibility to reach the lowest limit with 30kg of liquid Xe medium, in progress, will be installed and taking data at the UK Boulby Mine next year 2001. The current research and development program, including a pending NSF proposal, covers construction and operation of the 30-kg ZEPLIN II detector, which will cover most of the predicted SUSY regions. With supplemental funding from the DOE's advanced detector program, we will be able to confirm a new method to improve the detector energy threshold by means of photon amplification in liquid and gas Xe using CsI internal photo cathode.

Liquid noble gas time projection chamber (TPC) technology has been utilized for a couple of key frontier high energy physics experiments. The UCLA group participation at ICARUS experiment, using liquid Ar, as well as the liquid Xe Dark Matter detector R&D, has shown the capability that an independent research project for detector physics could be carried by qualified UCLA doctorate graduates and postgraduate students under the supervision of highly reputed senior physicists. For a better credential, the UCLA Dark Matter laboratory engineered the largest sized Dark Matter detector using two phase Xe (ZEPLIN II) in which we hope to find Galactic Dark Matter with the form of weakly interacting massive particles (WIMPs) in the mass range of 1 - 103 GeV.

In this proposal, we want to establish two objectives. One is to set a firm limit of electroluminescent photon amplification through the careful measurement of a proven amplification method, a CsI internal photo cathode in the two phase Xe chamber. The other is to apply the same method for the currently developed two-phase Xe detector (ZEPLIN II) for Galactic Dark Matter search. With the experimental setup in the gaseous Xe chamber at the CERN laboratory in Switzerland, the use of CsI internal photo cathode caused approximately 10 times overall amplification, taking CsI quantum efficiency into account. With repeated measurements of the experiment, the firm limit of amplification efficiency can be achieved for the two-phase detector. In order to set up the experiment to test the same amplification method for two-phase Xe chamber, we request funding to facilitate the operation of the test in UCLA Dark Matter laboratory.

It is very clear that two-phase Xe detector has a scientific and technological edge to detect the undiscovered Dark Matter particles in the future. In addition, it is very important that the US participation at the search of Dark Matter must be expanded to a larger scale. We believe that the proposed testing facility at UCLA will solidify the position of future US participation for the worldwide Dark Matter searches. With a successful test result and combining the ZEPLIN II system, it would be an ideal Dark Matter detector for the Carlsbad laboratory in the USA.

Table of Contents

ABSTRACT 1

TABLE OF CONTENTS 2

LIST OF FIGURE 3

1 PROJECT OBJECTIVES 5

2 INTRODUCTION 6

2.1 NEUTRALINO AS THE STRONGEST WIMP DARK MATTER CANDIDATE 6
2.2 CASE FOR NON-BARYONIC DARK MATTER AND EXPERIMENTAL EFFORTS 6
2.3 UNDERGROUND LABORATORY FOR LOW BACKGROUND 8

3 DETECTION PRINCIPLES AND DISCRIMINATION OF NUCLEAR RECOIL SIGNAL ... 10

3.1 ENERGY SPECTRUM, EVENT RATES, BACKGROUND DISCRIMINATION 10
3.2 STATISTICAL ENHANCEMENT OF DISCRIMINATION 10
3.3 LIQUID XE AS A DARK MATTER TARGET 11
3.4 NUCLEAR RECOIL DISCRIMINATION IN LIQUID XE 12
3.4.1 Single phase pulse shape discrimination 12
3.4.2 Proportional scintillation in single phase test chambers 13
3.4.3 Enhanced proportional scintillation using two-phase Xe 15
3.5 FORM FACTOR CORRECTION 17
3.6 BACKGROUND 19

4 THE ZEPLIN II DETECTOR 21

4.1 CENTRAL DETECTOR 21
4.2 XENON PURIFICATION 25
4.3 ELECTROLUMINESCENCE 27
4.4 STATUS OF ZEPLIN-II PROJECT 28

5 CSI INTERNAL PHOTOCATHODE FOR SIGNAL (PRIMARY SCINTILLATION) AMPLIFICATION 29

5.1 PRICIPLES OF CSI LUMINESENCE PLATE 29
5.2 INITIAL TEST RESULTS 34
5.3 PROPOSED TEST OF THE CSI LUMINESCENCE PLATE AT UCLA 35
5.4 PROPOSED R&D PROGRAM FOR PRIMARY SCINTILLATION PHOTON SIGNAL AMPLIFICATION 36

6 CONCLUSION 37

7 BUDGET & COMMENTARY 38

8 CURRENT AND PENDING SUPPORT STATEMENT 39

9 BIOGRAPHICAL SKETCHES 40

List of Figures

Figure 1 Summary of sensitivities in current running (CDMS & DAMA) and expectations from future experiments (CDMS & ZEPLIN-II). Curve labeled as ZEPLIN-IV shows the expected sensitivity with improved energy threshold (in this proposal) and scaled-up design, using scintillation techniques, showing objectives of the liquid Xe ZEPLIN program. The CDMS collaboration has similar objectives, using a cryogenic phonon+ionisation technique with semiconducting Ge & Si as targets (in the Soudan Mine, Minnesota from 2001). A muon veto is required for rates below 0.1/kg/d at Soudan, and for rates below 0.01/kg/d at the greater depth of the Boulby Mine. 9
Figure 2 Scintillation pulse shape difference between alphas and electrons in liquid Xe. 12
Figure 3 (a) single phase test chamber, (b) processes following collision, (c) S1 & S2 pulses for alpha and gamma interactions (the actual picture of (c) is shown in Figure 6) 13
Figure 4 Normalized primary and secondary scintillation vs. applied electric field for a 5.4MeV alpha. 14
Figure 5 Normalized primary and secondary scintillation vs. applied electric field for a 100keV gamma. 14
Figure 6 Waveform of alpha and 122keV gamma scintillation and proportional scintillation signal from PMT. P is referred as primary scintillation, and S as secondary scintillation 15
Figure 8 Two-phase test detector. 16
Figure 9 Primary and secondary scintillation vs. drift field with secondary under three different proportional fields with 122keV gammas. 17
Figure 10 Direct and shaped signals from a 22keV gamma. X-axis is plotted as the number of sampling points with 10 ns sampling rate. 17
Figure 11 Dimensionless figure of merit C(E) as a function of true recoil energy estimated from liquid Xe test results, compared with corresponding values for pulse shape analysis in NaI. Background rejection factor is $\sqrt{C/N}$ for N event in given energy range. 18
Figure 12 Nuclear form factor correction for Na, I and Xe recoils, plotted against gamma-equivalent energy. Note that for weakly interacting particles the Bessel function zeros will be smoothed for spin-dependent interactions, but will remain as large dips in the case of spin-independent interactions (in contrast to nuclear scattering of e or n) 19
Figure 13 3-D view of the ZEPLIN II Central Detector. Seven 5-inch PMTs are placed on a copper plate support. A PTFE cone is used to confine the liquid Xe with field shaping rings placed outside the Teflon. The luminescent-field structure is shown between top copper plate and the PTFE cone (wires are not shown) 23
Figure 14 The ZEPLIN-II cryogenic vacuum vessel. The center detector will be placed at the bottom of the inner vessel. Estimated thermal loss is about 10 watts. Feedthroughs for HV and signals as well as all pipelines are placed on top for easy installation and to minimize background 24
Figure 15 Drift field calculated with simplified model. Left: normal condition. Right: Charged up condition. Electrons will drift downwards. The tilted line is the boundary between the liquid Xe and the Teflon cone. 25
Figure 16 Electron lifetime measurements setup. Purified liquid Xe was filled in the chamber (left box). A laser pulse produces charges. The cathode box are specially made to shift the laser trigger noise. Charge leaving the cathode box and arriving at the anode are both measured with the same amplifier (right) 26
Figure 17 Lifetime measurement results. Electrons drift under an electric field of 10V/cm. The first big spike is the noise from the laser trigger. 26
Figure 18 Electron drift velocities under different drift fields E and temperature. Notice that the constant speed at ~ 250V/cm. 27
Figure 19 Primary verses Secondary plot in two-phase (top) and single-phase (bottom) Xe. 28
Figure 20 The UCLA Dark Matter lab. Figure 21 PTFE and copper plates 28
Figure 22 Typical *i-V* curves of the CsI photocathode measured in Liquid Xe and vacuum. (E. Aprile et al. NIM A343 1994, 129-134) 30

Figure 23 A picture of the CsI luminescence plate with an outer diameter of 66mm (the active CsI part is 50mm); the CsI is exposed in the inner circle (darker area in the picture).....30
Figure 24 CsI coating on the PCB board.....31
Figure 25 Pin array used to prevent CsI deposite in the holes during coating.....31
Figure 26 The CsI coating setup. It is then placed in a vacuum deposition chamber for coating at CERN.....32
Figure 27 The drift trajectory of photoelectrons (from bottom surface) and ionization electrons.....33
Figure 28 Electric field at the surface of CsI. Horizontal axis are the location on the plate. The vertical axis is the field normal to the surface in V/cm.....34
Figure 29 A simple diagram of the experimental setup of the CsI internal photo cathode for one phase Xe (left) and two-phase Xe (right).....34
Figure 30 Typical signals from the experimental setup with CsI internal photo cathode in the one phase Xe test chamber. Normal amplification signal (left) and when the gamma-Xe nucleus interaction occurs near the plate (right).....35
Figure 31 The conceptual drawing of ZEPLIN IV detector (500kg liquid Xe target) based on the ZEPLIN-II design and the expected CsI internal photocathode results. (Electronics and field shaping rings are not shown).....36
Figure 32 The proposed CsI internal photocathode test system with two-phase Xe at UCLA. (left) the actual test cell. (right) Vacuum thermal insulation chamber.....37
Figure 33 Conceptual drawing of the system setup.....37

1 Project Objectives

Since the on-going ZEPLIN II project (described below in detail) and CDMS II have currently the best possibility to reach the lowest limit of neutralino detection, they could be best viewed as an R&D for the ultimate scaled up liquid Xe dark matter detector. Although the ZEPLIN II detector has vastly been optimized for the maximum performance, there is room for developing a better method to lower the detector energy threshold and to reduce dead regions to keep a signal loss to the minimal and at the same time maximize the radioactive background rejection. In the case of ahieving lower detector energy threshold we developed a single gas phase liquid Xe test chamber with CsI internal photo-cathode for the primary scintillation photon amplification at CERN. A further study of this research effort should be carried for the current two-phase Xe detector with a better precision of the amplification. The project suggested in this proposal has, therefore, two major goals:

(1) Set a firm limit of electroluminescent photon amplification through the careful measurement of a proven amplification method, a CsI internal photo-cathode in the two-phase Xe chamber.

(2) Apply the same experimental method for the currently developed two-phase Xe detector (ZEPLIN II) as the R&D program of the ultimate scaled-up liquid Xe dark matter detector (500kg liquid Xe target). Also, reduce dead regions of the detector to the minimal using a computer analysis.

Our group's research efforts have been carried out extensively at CERN in collaboration with P. Picchi and the Torino group. Here, we request funding to establish the R&D facility (including a possible transfer of equipment from CERN) to achieve the outlined project objectives at UCLA, considering the significance of having these types of experiment in the US soil. We believe the proposed research program is crucial as the R&D program for the ultimate liquid Xe dark matter detector possibly at the WIPP site, Carlsbad, New Mexico.

The search for supersymmetric particle WIMPs may require a very sensitive detector capable of reaching 10^{-4} events/kg/day (or less) - this requires very powerful discrimination and a massive detector. **Figure 1** shows a range of models for SUSY WIMPs and the expected rates. Note that very low rates are possible in their models. We also show in **Figure 1** the expected sensitivities of CDMS II and ZEPLIN II. In order to improve the sensitivity of the liquid Xe detector we need to

(1) increase the mass (say to 500kg).

(2) reduce the energy threshold using the method proposed to be tested here (factor of 10 improvement in sensitivity is possible).

If both of these can be accomplished we may reach the level of sensitivity labeled as ZEPLIN IV in **Figure 1**. Note that this would be very complementary to CDMS II and could help confirm any signal CDMS II may claim in the near future using a totally different technique. For this reason we believe the amplification tests proposed here are very important for the ultimate search for dark matter WIMPs.

2 Introduction

2.1 Neutralino as the strongest WIMP dark matter candidate

The experimental search for cold dark matter is one of the most exciting challenges of the next few years, for both cosmology and particle physics. Increasing observational evidence continues to indicate that the majority of dark matter in galaxies and galaxy clusters is in a non-baryonic form. Moreover, the strongest theoretically suggested WIMP (Weakly Interacting Massive Particle) candidate exists in the form of the lightest supersymetric particle (LSP or 'neutralino' in this proposal) of supersymmetry theory, which would be formed in the early universe and subsequently clustered in Galaxies with normal matter. Scattering with normal matter would produce detectable nuclear recoils. Estimates of interaction event rates are in the range 0.001- 1 events/kg/d, the most favored region being 0.01 - 0.1 events/kg/d.

No experiments are yet running which could observe such low event rates. Intensive world development work has been in progress to reach a level of sufficient sensitivity to observe these theoricially proposed neutralino-normal matter interaction signals. Following such detection, a scaled up or an array of small detectors and other types of detector would constitute a 'dark matter telescope' to study the astrophysical properties of the dark matter (including density and Galactic velocity distribution) in addition to determining the basic particle properties (mass, spin-dependence, and etc.).

2.2 Case for non-baryonic dark matter and experimental efforts

The nature of the non-luminous matter in the universe continues to be a major unsolved problem at the interface of astronomy and particle physics. The motion of stars and gas out to >100 kpc allows the mass profile of the Galaxy to be estimated, and shows that the visible stars constitute only 10% of the Galactic mass, immersed in non-luminous matter which constitutes the other 90%. Similar conclusions result for other galaxies. The candidate explanations for Galactic dark matter are in two main classes

(a) Baryonic: e.g. non-luminous stars of less than 1 solar mass, referred to as MACHOs.

(b) Non-baryonic: e.g. new weakly interacting massive particles (WIMPs) or new light bosons (eg axions), light neutrinos.

Dynamical observations alone cannot distinguish between (a) and (b), but there are other observations which now strongly favor (b). In particular,

(i) The majority of dark halos in spiral galaxies are no known to extend to radii of at least 100-200 kpc. If baryonic (e.g. in the form of molecular hydrogen or ionized hydrogen as sometimes suggested), this would give a density parameter $\Omega_b > 0.1$, which would then exceed by a substantial margin the nucleosynthesis limit $\Omega_b = 0.4 \pm 0.2$ (Weinberg et al., 1998 ApJ, Copi et al., 1995 PRL 75, 3981) . This in itself is regarded by many astronomers as a convincing argument for non-baryonic dark matter as the dominant component of our Galaxy.

(ii) The behavior of off-axis visible matter and gas can be used to infer that the dark halos are not flattened like the baryonic disk, but are in the form of an ellipsoid of eccentricity ~ 3:1. This shows that the halo material did not relax into a disk, as would be expected if it is weakly interacting.

(iii) Measurements of the Suntaev-Zeldovich effect on the CMB can be used to estimate the electron density in galaxy clusters, and hence the corresponding baryon density. Latest results (Birkinshaw, IAU2000) show only 7±1% of the dark matter in clusters to be in baryonic form. Thus it is regarded as a firm conclusion that the

majority of cluster dark matter is non-baryonic. A substantial amount of this must also be in the individual galaxies, since these must contain at least a component due to infall from the cluster.

(iv) Searches for MACHOs in our Galaxy by gravitational lensing continue to see too few events to account for more than about 20% of the total Galactic dark matter .

The case for a particle explanation is thus now strengthened. The most experimentally accessible are the WIMPs, with the particular theoretical possibility of a lightest, stable, supersymmetric particle. At typical Galactic velocities (0.001c) these would be observable as keV-range nuclear recoils from elastic scattering in low background underground detectors.

Other classes of particle are more difficult experimentally, and perhaps also less favored theoretically. One experiment is in progress in the US to search for light axions, through conversion to microwave photons in a magnetic field. Light neutrinos are difficult to reconcile with galaxy formation models but remain possible in principle, requiring one neutrino to have a mass ~20 - 50eV. Because of their low energy (10^{-4} - 10^{-2}eV) these are not experimentally detectable in the foreseeable future, although a neutrino mass in the 10 - 50eV range is not definitively excluded and could be directly verified by time of flight from a supernova. Recent indications from SuperKamiokande of atmospheric neutrino oscillations appear to suggest a neutrino mass scale (< 1eV) too low to account for a significant fraction of the dark matter.

Supersymmetry continues to be an important candidate theory for accounting for a natural particle mass hierarchy. In particular, it predicts the existence of a lightest (stable) supersymmetric particle - the neutralino - with mass > 40GeV (from accelerator searches) and most probably < 200 GeV from theoretical considerations (Roszkowski 1997 Dubna workshop) Such particles would be created in large numbers in the early universe and would subsequently cluster in association with normal matter. The neutralino has thus become a leading candidate for the dark matter, with the merit that the theory makes order-of-magnitude predictions of the event rates expected in specific target nuclei. Dependent on model parameters, event rate estimates are in the range 0.001-1/kg/d, with the narrower range 0.01 - 0.1/kg/d most favored. For detailed discussions of supersymmetry and dark matter see Jungman et al. (1996 Phys Rep 267, 195), Kane et al. (1994 PRD 49, 6173), Treille (1994 RPP 57, 1137), Roszkowski (1997 Dubna workshop), Ellis (1991 Physica Scripta T36, 142), Nojiri & Drees (Phys Rev D48, 3483), Arnowitt & Nath (1995 MPL A10, 1257, PRL 74, 45992).

Nevertheless, experiments based on nuclear recoil cover a wider range of possible particles, since they are free from any assumptions about the nature of the particles or their theoretical basis. The outcome of low energy scattering from a nucleus depends purely on kinematics, and the expected nuclear recoil spectrum follows in a simple way from the incident and target masses, together with the expected Galactic velocity distribution. Thus any particle in the 10 - 1000 GeV mass range, including a heavy neutrino for example, would be detectable in these experiments.

An additional consideration is that some types of interaction may be spin-dependent, so it is important to include target nuclei with non-zero spin. In the case of the neutralino a mixture of spin-dependent and spin-independent interactions is expected, so that any target material should be sensitive to such particles. In the spin-independent case, the rate for low momentum transfer will be proportional to the square of the number of neutrons and/or protons in the nucleus (for example only neutrons contribute significantly in the case of Dirac neutrinos) but with increasing recoil energy the inverse momentum transfer (fermi) becomes comparable to or less than the nuclear radius and all interaction rates are reduced by a form factor correction (see below). This provides an important incentive for achieving the lowest possible detection energy threshold, which in addition maximizes the fraction of events collected for a wide range of particle masses.

In the event of observation of a positive signal there are in principle two methods of proving this to be of Galactic origin. The first would be to scale-up to a sufficiently large target mass (typically >100kg) to observe the annual modulation in rate and energy spectrum arising from the motion of the earth around the sun, combined with the sun's motion through the Galaxy. The mathematics of these results in a ± 5% rate modulation (dependent on energy threshold) with a maximum in June and minimum in December. The second possibility is to develop a detector capable of measuring recoil direction, for which there is a typical 4:1 forward:back ratio relative to the direction of motion through the Galaxy, so that the earth's rotation gives a diurnal modulation an order of magnitude larger than the annual modulation. Because low energy recoils have a short range (~1-5 $\mu g/cm^2$) directionality will require sub-micron target layers, or low pressure gas detectors to record recoil direction as tracks, and hence observe individual events correlated with Galactic motion.

In either case it is essential that the events are shown specifically to be nuclear recoils. A recent claim by the DAMA (Rome) collaboration to have observed seasonal modulation in count rate from NaI crystals has the defect that the modulation is observed in the total count rate - which includes gamma, beta and alpha background (plus any systematic error including that observed in the UK NaI detectors) and is also close to the electronic noise threshold. There is no analysis offered to show the modulation as a function of pulse shape. Our ZEPLIN II detector will search for seasonal modulation specifically in an identified population of nuclear recoil events (with neutron events excluded) and hence would be definitive.

Figure 1 shows the expected sensitivity of the ZEPLIN-II detector along with other world programs, notably the CDMS cryogenic experiment to be installed in the Soudan Mine, have similar objectives.

2.3 Underground laboratory for low background

In order to keep the level of background noise from the already known particles (neutron, gamma, alpha, beta and etc.) as low as possible, a deep underground laboratory to facilitate any developed detector is necessary with a large veto system. In a deep underground location, neutron background can be reduced to a level below the expected event rate so that observation of nuclear recoil events would provide clear evidence of a flux of new neutral particles. Since the majority of detector types will also detect electron recoils, it is also essential to devise methods which discriminate between nuclear recoil events and beta & gamma background.

For the ZEPLIN II detector, we chose the UK Boulby Salt Mine for the installation. Our UK collaborators for the ZEPLIN II project have been developing excellent facilities and infra-structure for dark matter searches in the 1100m deep Boulby Mine. Low backgrounds have been demonstrated in the initial program based on pulse shape discrimination in NaI crystals. The UK program has now been funded to include liquid Xe targets, and a preliminary small Xe detector (5kg target) using only pulse shape discrimination has been installed underground with its associated cryogenic, purification, and safety systems.

The UK and US programs are now formally linked by an MOU, in which the combined expertise of the two groups would be used to construct and operate a scaled up version of the proven UCLA test chamber, with liquid Xe mass 30kg and referred to as ZEPLIN II. The initial hardware funding for this, including a surrounding veto and shielding system, is being provided largely by the UK. The key central chamber is under construction by UCLA/Torino.

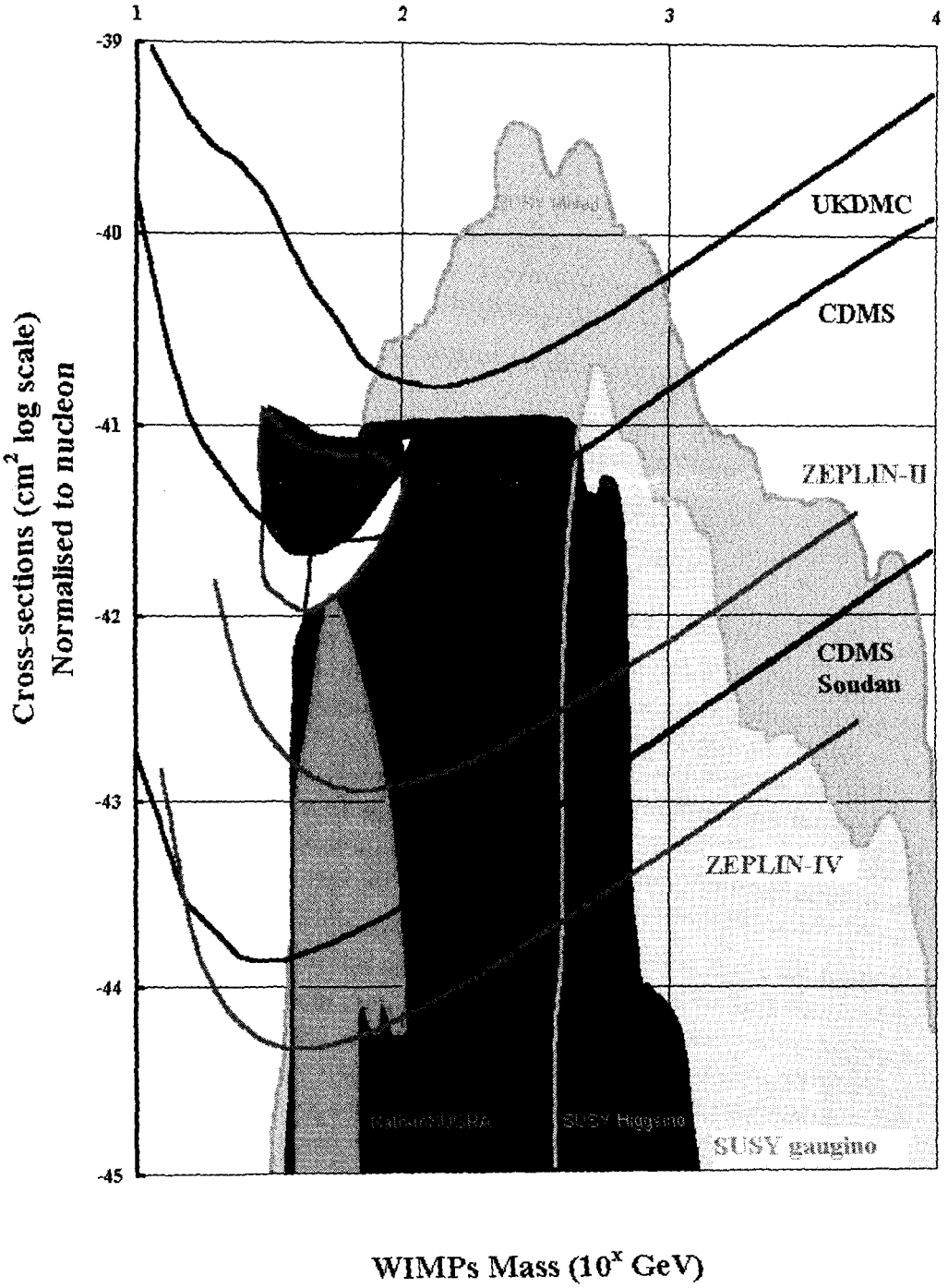

Figure 1 Summary of sensitivities in current running (CDMS & DAMA) and expectations from future experiments (CDMS & ZEPLIN-II). Curve labeled as ZEPLIN-IV shows the expected sensitivity with improved energy threshold (in this proposal) and scaled-up design, using scintillation techniques, showing objectives of the liquid Xe ZEPLIN program. The CDMS collaboration has similar objectives, using a cryogenic phonon+ionisation technique with semiconducting Ge & Si as targets (in the Soudan Mine, Minnesota from 2001). A muon veto is required for rates below 0.1/kg/d at Soudan, and for rates below 0.01/kg/d at the greater depth of the Boulby Mine.

3 Detection Principles and Discrimination of Nuclear Recoil Signal

In order to better describe our proposed R&D work for two-phase Xe detector for the dark matter search, understanding principles of basic detection scheme and discrimination methods for nuclear recoil signal is necessary. We summarize them in the following.

3.1 Energy spectrum, event rates, background discrimination

The nuclear recoil signal is expected to be in the form of a continuous spectrum with differential counting rate (events/keV/kg/day) as a function of recoil energy E_R (keV) approximated by

$$dR/dE_R = c_1 (R_o / E_{or}) [\exp (-c_2 E_R/E_{or})] [F(E_R)]^2 \qquad (1)$$

where $r = 4M_DA/(M_D+A)^2$ for target element A and incident particle mass M_D , $E_o = M_D v_o^2/2$ (v_o = Galactic velocity dispersion ≈ 210 km/s, E_o converted to keV) and F^2 is a nuclear form factor correction. There may be further correction factors to allow for detection efficiency and the fraction of a given element in a compound target (e.g. only about 50% of a Xe target has nuclear spin). The coefficients $0.5 < c_1, c_2 < 1$ provide a convenient way of modifying the formula for the motion of the earth relative to the Galaxy. For a stationary earth, $c_1 = c_2 = 1$ giving total event rate R_o. The motion of the sun modifies this to $c_1 \approx 0.78$, $c_2 \approx 0.58$ with further ±5% annual variations arising from the orbital motion of the earth (for a full discussion of the mathematics of dark matter experiments see Smith & Lewin, Astroparticle Physics 6 (96) 87).

Thus a limit on, or measurement of, the differential rate dR/dE_R for a given E_R leads to a corresponding limit or value for R_o for each assumed particle mass M_D. This is the basis of the limit curves in **Figure 1**, the minimum of the curves occurring approximately when $M_D \approx A$. Because the above spectrum falls sharply with energy, a low energy threshold (< 10 keV) is important. Moreover, scintillation detectors will in general respond to nuclear recoils with a light output which is less than the electron or gamma-equivalent energy. This relative scintillation efficiency, or 'quenching factor' f_A, has to be measured for any target element A by using neutron scattering to produce the nuclear recoils. The importance of this is that a detector is calibrated with gammas (electron recoils) then any nuclear recoil event of observed energy E_{obs} corresponds to a true recoil energy $E_R = E_{obs} / f_A$ and it is this value which applies throughout eq.(1). Examples of well-established measured values of f_A are ~ 0.3 for Na in NaI, and ~ 0.09 for I in NaI. Recent measurements of f_A for Xe by this collaboration, using neutron beam facilities at Legnaro, Italy and at Sheffield, have given the value $f_{Xe}= 0.22 \pm 0.02$ The recoil efficiency affects experimental sensitivity in particular through the form factor correction, which follows approximately a Bessel function in qR_A where R_A = nuclear radius and momentum transfer $q \approx \sqrt{(2AE_R)} = \sqrt{(2AE_{obs}/f_A)}$. Form factors are discussed further in **§3.5**.

The left hand side of eq. (1) will contain the detector background plus any signal. Discrimination in liquid Xe allows an upper limit to be placed on the signal content as a fraction of background events. Substitution of this upper limit on the left side of eq. (1) then allows an upper limit on R_o to be plotted as a function of the hypothetical particle mass M_D.

3.2 Statistical enhancement of discrimination

There will in general be an overlap between signal and background event distributions as a function of some discriminating parameter p (such as pulse time constant). A 'cut' on p to include, say, 90% of the signal events, will also include some (energy-dependent) fraction f_g of

misidentified background events. Thus a straight 'cut' to the data would be limited to a factor f_g gain in sensitivity. However much larger gains are possible by statistical analysis of a long run of data. By calibrating a detector with gammas and neutrons, event distributions for nuclear recoils and gammas can be obtained as a function of energy and of the discriminating parameter p.

These are determined separately for discrete energy intervals E_1 to E_2 (typically a few keV) and will in general vary slowly with energy, determined from the calibration data. For zero nuclear recoil signal, the experimental background distribution is expected to coincide with the gamma calibration distribution. An upper limit to the signal can then be estimated from the 90% confidence level fluctuations on the background, giving a 90% confidence level for the ratio of signal events S to background events N:

$$S/N \leq C\, N^{-0.5} \quad \text{with} \quad C = 1.3\, [f_g\,(1-f_g)]^{0.5} / [f_n - f_g] \quad (2)$$

where f_n , f_g are the fractions of nuclear recoil and gamma events below some value of p.

Thus the signal sensitivity in events per unit time improves not only linearly with reduction in background rate but also inversely as the square root of the number of counts in any specified energy interval. The numerical factor C which can be called a 'coefficient of discrimination'. From the distributions in p a value of p can in general be found for which C is optimum (i.e. minimum). This provides a basic 'figure of merit' with which to compare discrimination techniques. With actual data from an operational experiment a full chi squared analysis can be used to place a limit on the existence of a second population, but the use of the discrimination coefficient C provides a convenient means of assessing in advance any given technique or experiment.

3.3 Liquid Xe as a dark matter target

Liquid Xe satisfies the following basic requirements for a dark matter target:

(a) It is available in sufficiently large quantities with high purity.

(b) It scintillates via two mechanisms, responding differently to nuclear and electron recoil events.

(c) It contains both odd and even isotopes, suitable for spin-dependent and scalar interactions, offering the possibility of using enriched odd or even isotopes to identify the type of interaction.

(d) Its high atomic number provides a good kinematic match to the most theoretically-favored particle mass range 100-200 GeV.

Target masses 100-300kg may be needed to reach the lowest predicted event rates. The 30kg detector proposed in the ZEPLIN-II (under construction now) project represents a major step towards this, being a factor >10 larger than previous test chambers built at CERN and could subsequently be replicated to give a total target mass 100-1000kg. This would achieve sensitivity to the lowest neutralino event rates (0.001-0.01/kg/d) and could also detect the annual signal modulation which would confirm the Galactic origin of any signal.

The need for detectors based on a new target material and principle is highlighted by recent unexplained results. Following initial signal limits set by underground Ge detectors, some significant advances in sensitivity were made initially by means of pulse shape discrimination in low background NaI scintillating targets. Recently both the Rome and UK groups have encountered signal-like anomalies at the level 0.5-1 events/kg/d. Rome report a seasonal modulation of total count rate, while the UK see a separated population of recoil-like pulses. We

believe both have natural explanations (e.g. a source of low energy alphas) but this emphasizes the need for new detectors with higher sensitivity with different target elements.

With liquid Xe, signal discrimination can be achieved in two basic ways:

(1) By analyzing the total scintillation pulse shape - which differs by a factor ~2-3 in time constant for nuclear recoil and electron recoil events.

(2) By applying an electric field to inhibit recombination and (a) measuring the 'primary scintillation' S1 and (b) drifting the ionization component into a strong electric field in the anode region to produce a 'secondary scintillation' signal S2 with a time delay of up to 60 μs (100 mm drift).

Method (2) is more powerful , involving a comparison of two distinct signals associated with each individual event. The mean of the ratio S1/S2 differs for nuclear recoil and electron recoil events and provides the parameter p in §**3.2**, leading to a statistical signal/noise of order $\sqrt{(C/N)}$ where N is the number of background events and C is typically ~1% at a gamma energy of 10 keV. Sensitivity thus progressively improves by extended running (and larger target masses) subject to the elimination of any systematic errors that may be encountered.

Discrimination between alphas and gammas using this technique was demonstrated in 1994 by members of the ICARUS collaboration including the UCLA and Torino groups. Further tests used neutron scattering confirmed for the first time (a) that liquid Xe will give a scintillation response to recoil of its own nuclei, and (b) that the above discrimination processes remain effective down to energies < 5-10keV, as required for a dark matter experiment.

3.4 Nuclear recoil discrimination in liquid Xe

3.4.1 Single phase pulse shape discrimination

An extensive literature on basic excitation mechanisms in liquid Xe has shown that Xe_2^* excited states are produced which decay with two time constants 3ns and 27ns, emitting 175nm photons. In addition an ionized state Xe_2^+ is produced which can recombine to Xe_2^* and decay as before. The proportions of these decay processes is different for excitation by electrons (from gamma interactions) and alphas (equivalent to nuclear recoil) giving effective pulse decay times ~ 45ns for gamma interactions and ~ 15ns for alphas (**Figure 2**). These results are for small scale laboratory tests. In the past year, tests in the UK on a 5kg single phase Xe have shown that these results can be approximately reproduced on a larger scale. A ^{60}Co source was used to produce gamma interactions and an Am-Be source was used to produce a mixture of neutron and gamma interactions. Pulse analysis showed a time constant in the region 40ns for gamma interactions and ~20ns for neutron interactions, in reasonable agreement with the published small scale tests.

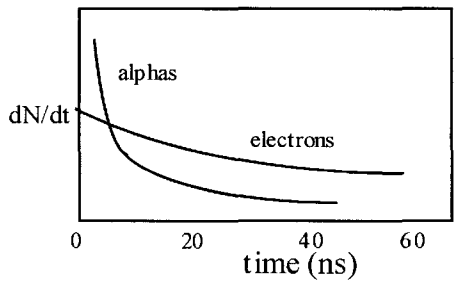

Figure 2 Scintillation pulse shape difference between alphas and electrons in liquid Xe.

3.4.2 Proportional scintillation in single phase test chambers

If an electric field is applied, the recombination process in §**3.4.1** is inhibited, and the ionization can be drifted into a stronger field to produce a second scintillation pulse, proportional to the amount of ionization. Thus a double scintillation pulse is produced - a primary pulse S1 from the initial excitation, followed a few 10s of μs later by a secondary scintillation pulse S2 from the drifted charge. From published data on the interaction of electrons, protons and heavy ions with liquid Xe, the ratio S1/S2 is predicted to be 0.1 - 0.3 for incident nuclei and 1-10 for electrons, with an overlap between these estimated to be only a few % at 10 keV.

These expectations were confirmed by tests carried out at CERN by members of the ICARUS collaboration, in particular H. Wang of UCLA. To demonstrate the basic principle, a small (50g) liquid Xe chamber, containing an electric field and coupled to a photomultiplier was irradiated with 5 MeV alphas and 120 keV gammas. Drift voltages of several kV suppressed recombination and a secondary scintillation signal was produced (see **Figure 3**, from Benetti et al., NIM A327(1993) 203). The ratio S2/S1, as shown in **Figure 4** and **Figure 5**, was >1 for gammas and <1 for alphas, as predicted. Subsequently, the double pulses were observed also with a larger (1kg) chamber and two coincident photomultipliers.

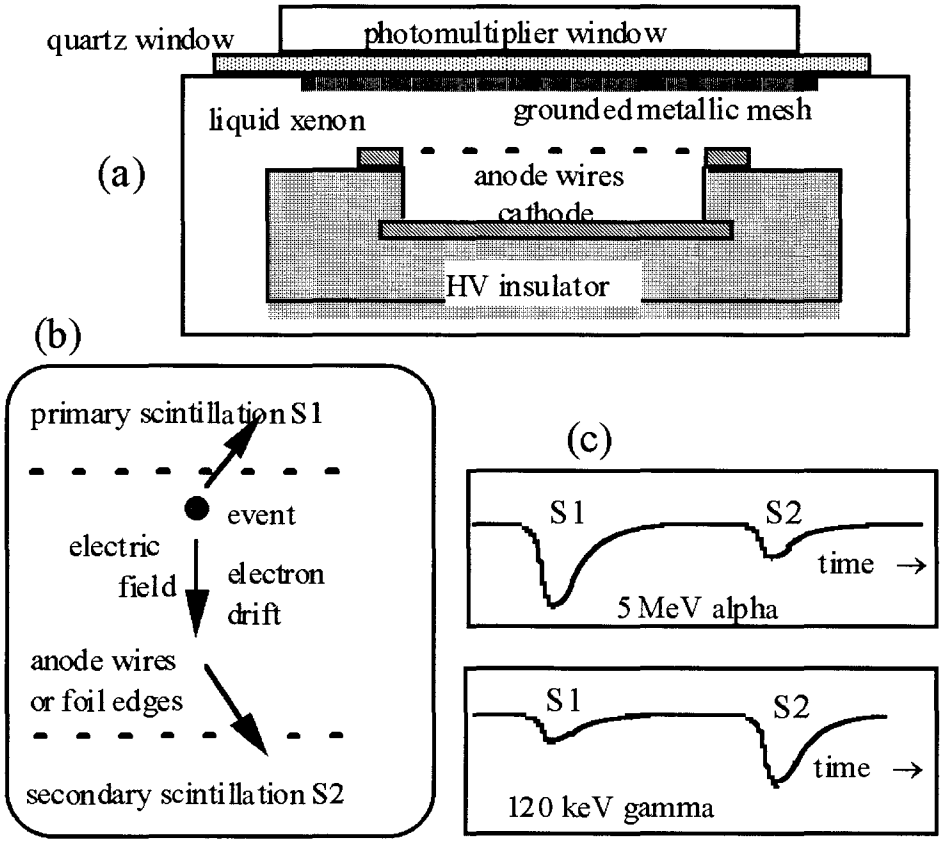

Figure 3 (a) single phase test chamber, (b) processes following collision, (c) S1 & S2 pulses for alpha and gamma interactions (the actual picture of (c) is shown in **Figure 6**).

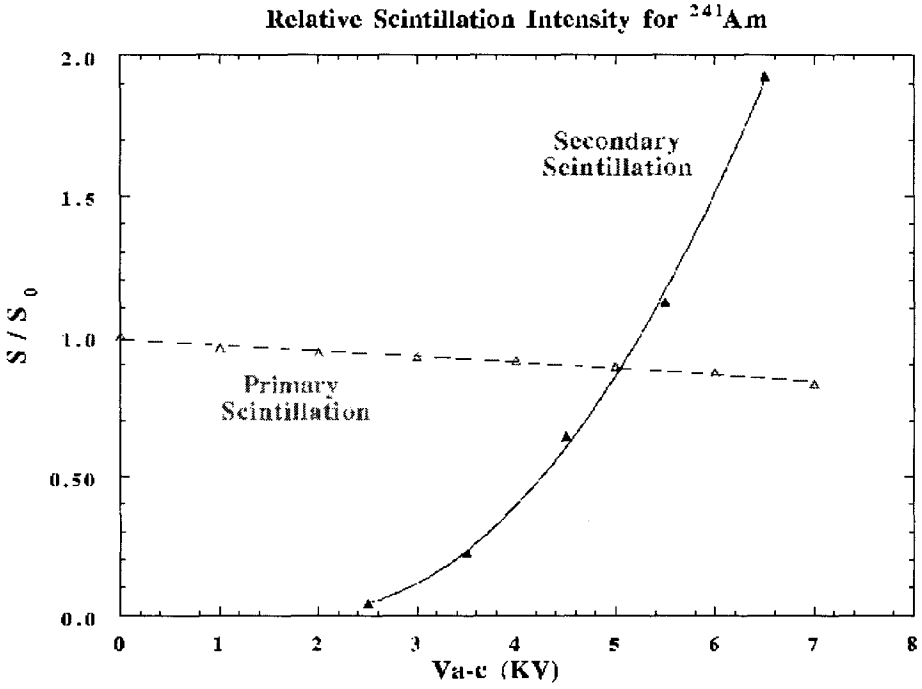

Figure 4 Normalized primary and secondary scintillation vs. applied electric field for a 5.4MeV alpha.

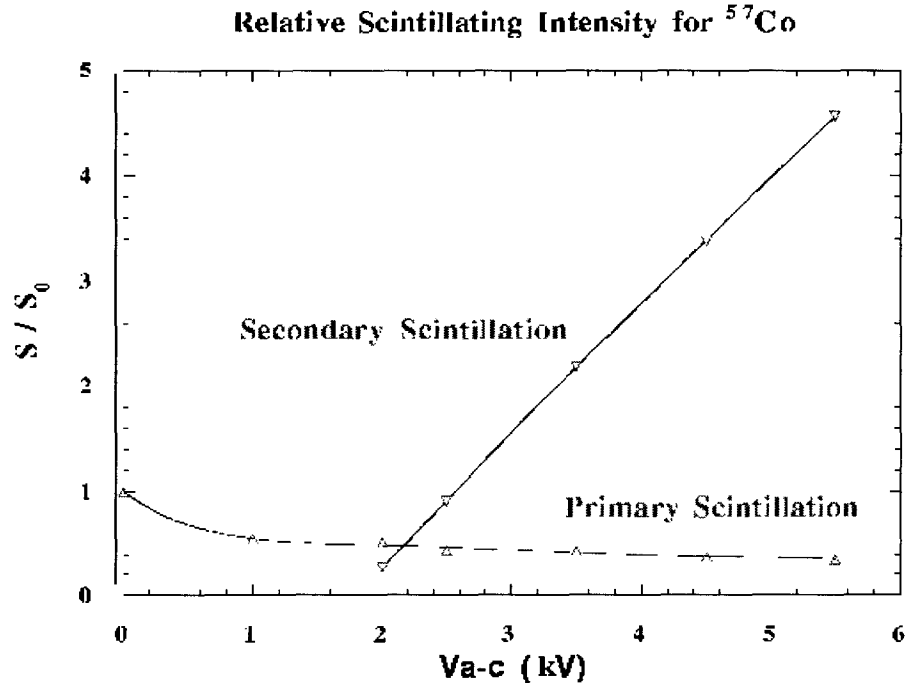

Figure 5 Normalized primary and secondary scintillation vs. applied electric field for a 100keV gamma.

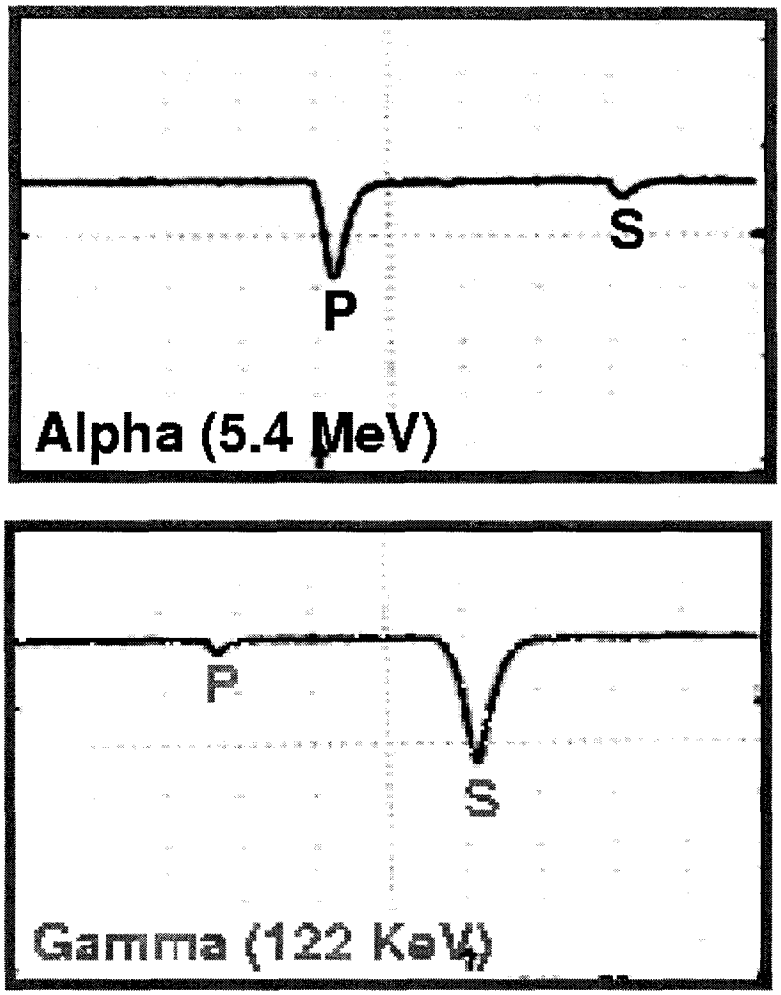

Figure 6 Waveform of alpha and 122keV gamma scintillation and proportional scintillation signal from PMT. P is referred as primary scintillation, and S as secondary scintillation.

3.4.3 Enhanced proportional scintillation using two-phase Xe

In 1997 an important improvement was made to this technique. By introducing a liquid surface into the chamber, with the electric field extending into the gas phase, the charge can be pulled into the gas and accelerated to give a much larger proportional scintillation signal, while the primary scintillation pulse remains unchanged. This improves background rejection in two ways:

(i) Since the nuclear recoils produce relatively little ionization, a larger difference between signal and background events is created.

(ii) Most background events are effectively amplified out of the low energy region and can be rejected by a cut on total signal amplitude.

Figure 8 shows a 0.5kg test chamber recently constructed using the two-phase principle. Initial test results are shown in **Figure 7**, in which the relative values of signals S1, S2, defined above, are plotted for events from an Am-Be source (which emits both neutrons and gammas).

The separation of nuclear recoil events (from the neutrons) and Compton scattering events is clearly demonstrated and is in accordance with expectation from the principles discussed above. An energy calibration of the neutron events was made from a Monte Carlo simulation using the known Am-Be source spectrum, which when matched to the observed event number distribution provides the energy scale shown in **Figure 7**. This is also consistent with simple kinematic estimates.

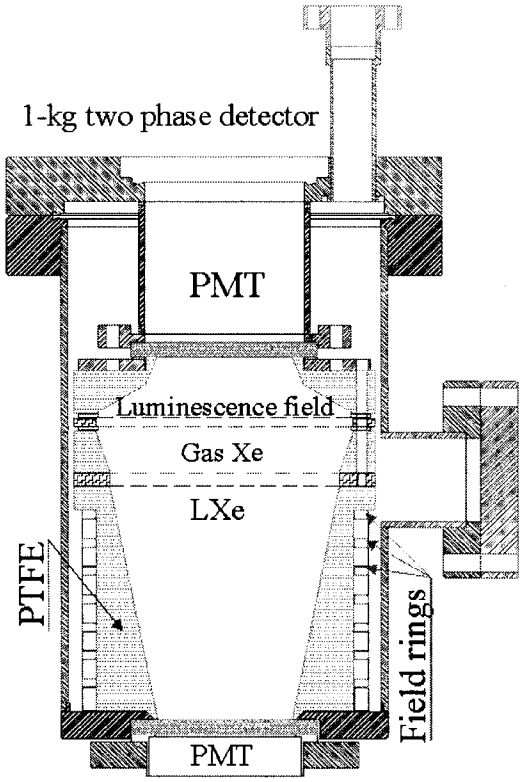

Figure 8 Two-phase test detector.

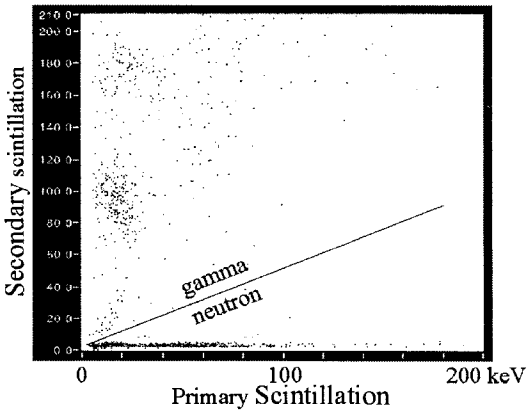

Figure 7 Separation of nuclear and electron recoils into two populations by primary and secondary scintillation in two phase system.

With the setup shown in **Error! Reference source not found.**, the drift and proportional fields are isolated. This means that by varying drift or proportional field, one can control the extraction and drift of the ionization electrons independently from the control of proportional gain. The test results of the separation are shown in **Figure 9** in single phase (liquid). Notice that the primary scintillation decreases with increased drift field because of the recombination decrease. At 250V/cm, the secondary scintillation pulse height under 2.5 kV (potential on the 3μm diameter wire) proportional field is already higher than that of primary scintillation. It is a perfect match with the constant electron drift velocity as shown below in §4.2, while, in the case of electroluminescence, the secondary is much higher. See §4.3. **Figure 10** shows a direct waveform of a 22keV signal from PMT taken from this set up.

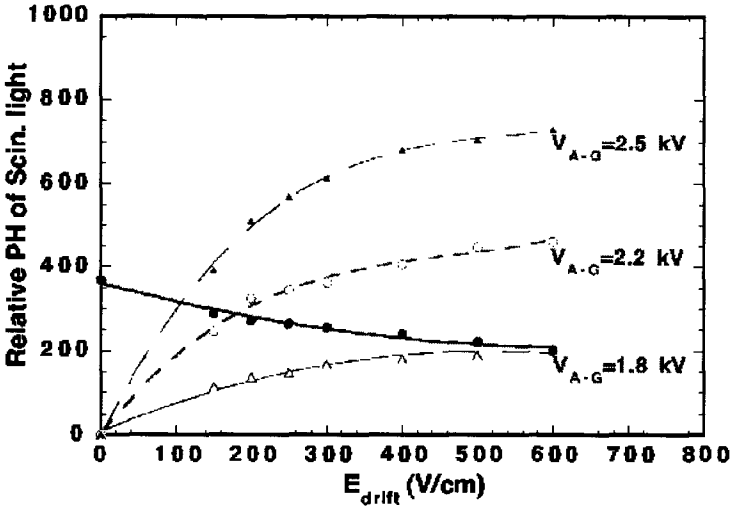

Figure 9 Primary and secondary scintillation vs. drift field with secondary under three different proportional fields with 122keV gammas.

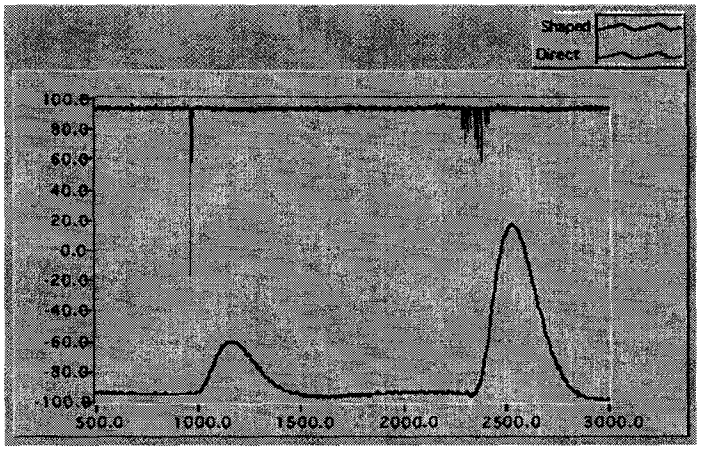

Figure 10 Direct and shaped signals from a 22keV gamma. X-axis is plotted as the number of sampling points with 10 ns sampling rate.

From these initial tests it is thus possible

(a) to conclude that the neutron and gamma events are separated down to < 10 keV actual recoil energy and

(b) to estimate approximately the neutron/gamma separation (i.e. the fraction gamma events overlapping with 90% of neutron events) as a function of energy (**Figure 11**) showing a factor ~10 improvement over the corresponding overlap achieved using NaI pulse time constant differences.

3.5 Form factor correction

The discrimination gain has to be considered in conjunction with the form factor correction, plotted in **Figure 12** as a function of true recoil energy. This shows the importance of achieving an observed energy threshold as low as 5 keV, corresponding to a recoil energy of 23 keV. Performance is best estimated by a direct comparison between Xe detectors and existing scintillation detectors based on NaI (and for which the achieved event rate sensitivity is known). From the viewpoint of coherent interactions we can consider just the I component of the NaI

(since it is 80% of the mass and has an A^2 factor 30 times higher). Moreover Xe and I have similar size nuclei, and hence similar form factor corrections for a given recoil energy. Xe gains over I in NaI for the following reasons:

(i)The recoil efficiency is higher for Xe (22%) than for I in NaI (9%), so will be sensitive to a lower recoil energy for a given energy threshold.

(ii)The discrimination factor and figure of merit C is better for Xe by an order of magnitude (**Figure 11**).

(iii)The intrinsic background in Xe (with sufficiently reduced ^{85}Kr) will be lower than that in NaI due to contamination with U and Th (for which significant reduction has not been achieved, despite efforts to do so).

Taking account of these three factors, and allowing for the factor 2 lower scintillation light output from Xe, simulations suggest a possible gain factor 100 in potential sensitivity of Xe detectors compared with NaI detectors. Since the latter have achieved a sensitivity level ~ 1 event/kg/day, this indicates that two-phase Xe detectors are in principle capable of achieving sensitivities down to 0.01 events/kg/day for the same mass and running time, and below that if scaled up to larger mass.

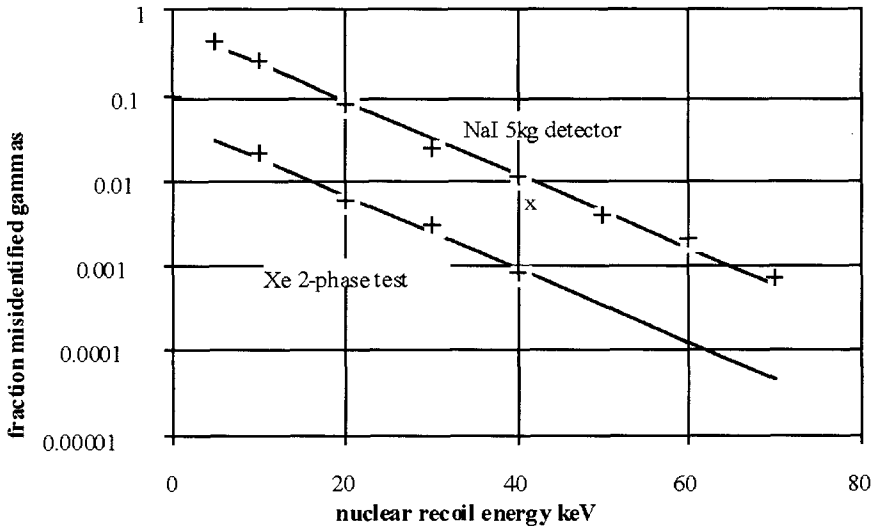

Figure 11 Dimensionless figure of merit C(E) as a function of true recoil energy estimated from liquid Xe test results, compared with corresponding values for pulse shape analysis in NaI. Background rejection factor is $\sqrt{C/N}$ for N event in given energy range.

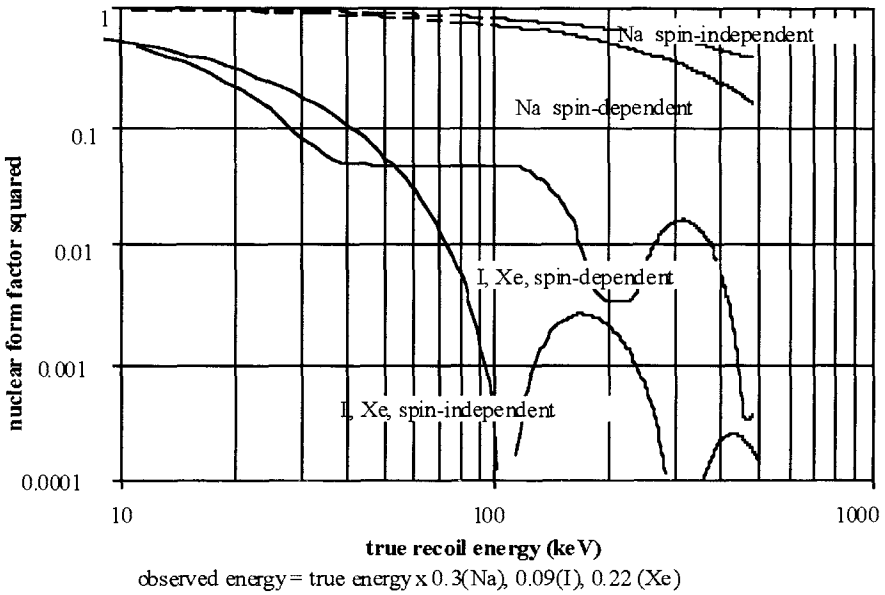

Figure 12 Nuclear form factor correction for Na, I and Xe recoils, plotted against gamma-equivalent energy. Note that for weakly interacting particles the Bessel function zeros will be smoothed for spin-dependent interactions, but will remain as large dips in the case of spin-independent interactions (in contrast to nuclear scattering of e or n).

3.6 Background

The basic feature of the detector is that it is able to discriminate between a nuclear recoil signal and background events from gammas and betas, with some overlap which can be reduced statistically by longer running and or a larger target mass. However, low energy nuclear recoils can also be produced by neutron interactions, so it is of prime importance to ensure that these are reduced to below the expected neutralino signal level. Nuclear recoils in the range 1-30 keV can arise from neutrons in the range $E_n = 0.1 - 10\,\mathrm{MeV}$. There are three main sources of neutron background:

(1) U and Th in the rock produce neutrons mainly via alpha interactions with the rock elements. The predicted rates in an underground cavern are typically a factor 10^5 lower than the background gamma flux (i.e. typically $10^{-6}/\mathrm{cm}^2/\mathrm{s}$). These neutrons can be thermalized and absorbed by hydrogenous materials giving a factor 10 attenuation per 20cm shielding.

(2) Within the shielding, further neutrons can arise from U and Th in the target and detector materials, but again at only 10^{-5} of the local gamma flux. The achieved gamma flux at Boulby after shielding is of order 100/kg/day, part of which may arise from U/Th contamination. Thus the neutron background from this must be < 0.001/kg/day. This would be reduced further with development of higher purity materials.

(3) Cosmic ray muons produce neutrons in all materials by both spallation and capture. From the cross section and multiplicity of those processes, and the muon flux, the neutron production cross section can be estimated as a function of depth. A Monte Carlo simulation gives a rate in a shielded target ~0.01 event/kg/day below 20keV at the Boulby mine. This is already low for the present experiment

and could be further reduced by a muon veto. This could be done with > 99% efficiency, reducing the muon-produced neutron events to 0.0001 event/kg/day.

Gamma and beta background should also be as low as possible, in order that the discrimination factor acts on a lower starting value and reaches the lowest possible signal level.

More important sources of background in this experiment are U and Th in the photo-multipliers, and intrinsic beta decay in the target materials, e.g. ^{85}Kr in Xe. Typical current ^{85}Kr contamination for 20ppm purity Xe gas is $5x10^{-17}$atom/atom, giving a low energy beta decay rate of ~50 event/keV/kg/day. However, this can be reduced by cryogenic distillation or by centrifuging.

The UK Boulby Salt Mine of our choice is a working mine at a uniform level of 1100m, with a network of many km of underground tunnels and caverns. The natural radioactivity is at least as low as any other world underground site, and background from this is further shielded as discussed above. Several adjacent caverns and tunnels are dedicated to the UK dark matter program. Full electrical services, telephone and fiber optic data links are installed, and the UK contribution to this project will include installation and manpower for commissioning, continuous running and data acquisition.

4 The ZEPLIN II Detector

Based on the R&D experience over the part years, we are confident that a two-phase Xe detector is the best for a WIMP dark matter search to cover the current interested SUSY region. The center detector is currently under construction at UCLA and active veto, shielding will be provided by Columbia and UK dark matter group. We describe the design of the ZEPLIN II detector below. The future large scale detector (ZEPLIN-IV) will have the same overall structure.

4.1 Central Detector

The key to the background rejection power in this detector, as described above, is the observation of the ionization components of the background events by looking at the luminescent photons produced by the ionization electrons in the Xe gas phase. Hence the collection efficiency of these ionization electron must be close to 100%. Any background event in the detector must not loose its ionization charges. Otherwise, it will be miss identified as a recoil event. With this in mind, the detector has the shape as shown in **Figure 13**. 100% of the active Xe used is confined to the region within which, ionization electrons will drift up to the liquid and gas phase surface. An extraction field is present at the surface so that electrons will continue to drift into the gas phase. Electron drifting in the gas regain will under go the electroluminescent process and produce over 200 photons per electron (discussed in details in §4.3). To avoid photon loss due to window materials, all seven PMTs are placed inside the vacuum vessel for better light collection efficiency. So PMTs will face directly to the scintillation photons. The PMTs are held by a copper plate above this luminescence region. Teflon spacers are used to both isolate the PMTs from the copper plate and block all scintillation photons from above the copper plate. This is to prevent the photons from the background events in the gas region in the upper part of the detector from entering the PMT readout.

The 3-D view and outer view of the detector is shown in **Figure 13** and **Figure 14**. A frustum shaped cup made by Teflon (PTFE) confines the active liquid Xe. Electric field shaping rings are placed outside the PTFE to avoid a fringing field effect on the ionization charge.

Special care are taken at all boundaries near the active region and wire frames, where the drift field for ionization electrons is configured such that all electrons must drift to the gas electroluminescence region. For regions (dead region) where it is imposible to form such drift field, have been reduced to less than 0.5% of the total active volume. **Figure 15** shows the static electric field near the Teflon as well as a charged up condition in this setup. The surface charge in this calculation is arbitrary and is only intended to show the effect of the charge up. As shown in the figure, it is clear that the charge up effect tends to modify the equipotential line such that in the worst case the equipotential lines will be perpendicular to the PTFE surface. Be cause once the equipotential lines are perpendicular to the surface, ions will move only in the direction parallel to the PTFE surface. The actual charge up will depends on the liquid Xe purity and the PTFE surface conductivity. The higher the Xe purity, the longer the ions stay on the surface. The ions will be carried away by the surface current be cause the conductivity of the PTFE surface is non-zero. The charge up will obviously distort the event location near the surface. The background rejection power does not depends on tracking and location of the event. So even the worst charge up condition happens, it will not degrade the capability of the detector.

Two wire frames are used to generate the electron extraction field and electroluminescence field. One of the wire set is placed in the liquid and the other in the gas phase. The strong field (>2.5kV/cm) between the two wire set is enough to extract electrons near the surface. Once electrons get out of the surface, they will under go electroluminescence process under this field.

The center detector is housed by a double layer vacuum vessel as shown in **Figure 14**. The estimated thermal loss is about 10 watts. It is important to keep the thermal loss low for safety

and low operation cost. A low power cooling system will be used to keep the system at liquid Xe temperature.

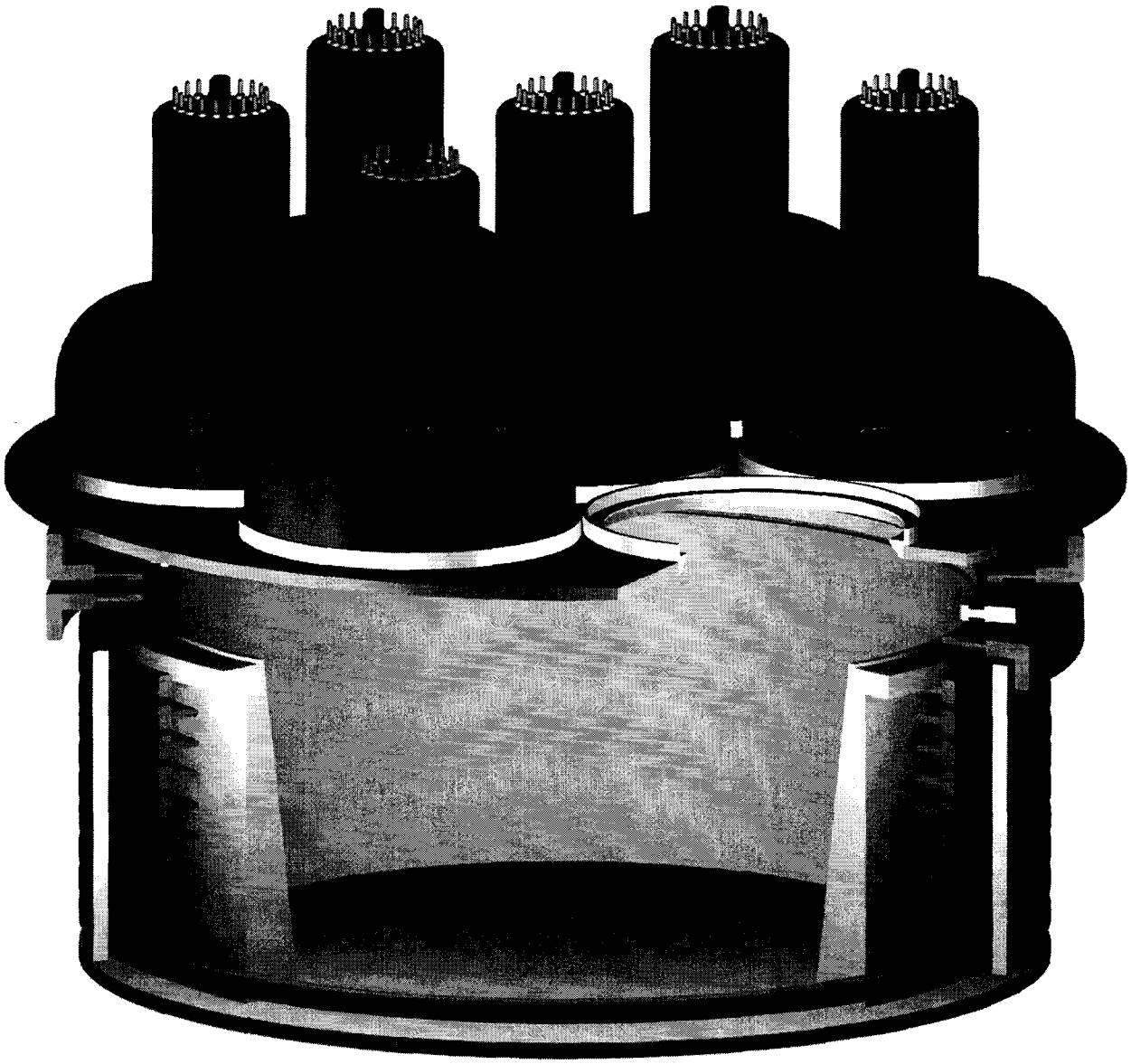

Figure 13 3-D view of the ZEPLIN II Central Detector. Seven 5-inch PMTs are placed on a copper plate support. A PTFE cone is used to confine the liquid Xe with field shaping rings placed outside the Teflon. The luminescent-field structure is shown between top copper plate and the PTFE cone (wires are not shown).

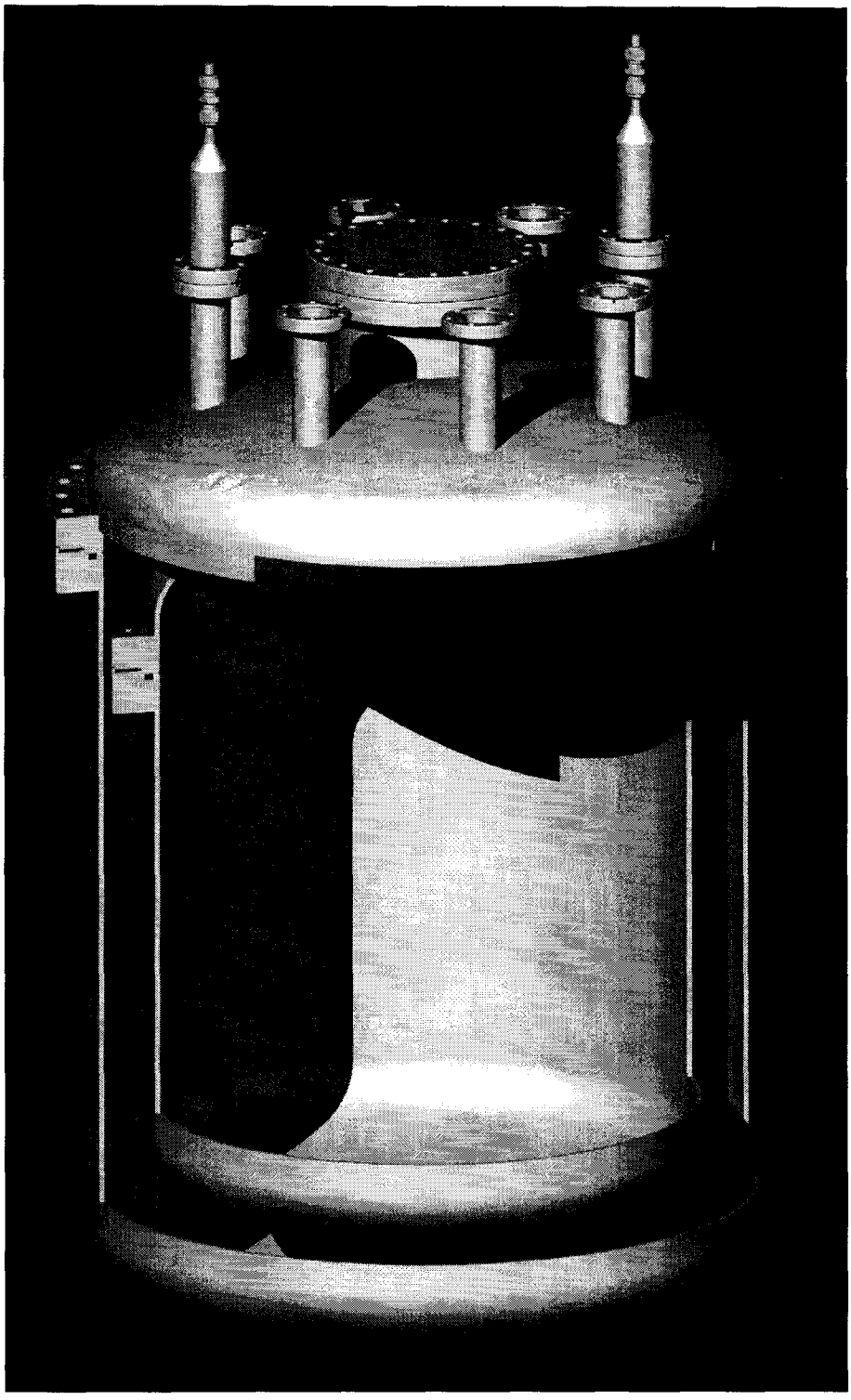

Figure 14 The ZEPLIN-II cryogenic vacuum vessel. The center detector will be placed at the bottom of the inner vessel. Estimated thermal loss is about 10 watts. Feedthroughs for HV and signals as well as all pipelines are placed on top for easy installation and to minimize background.

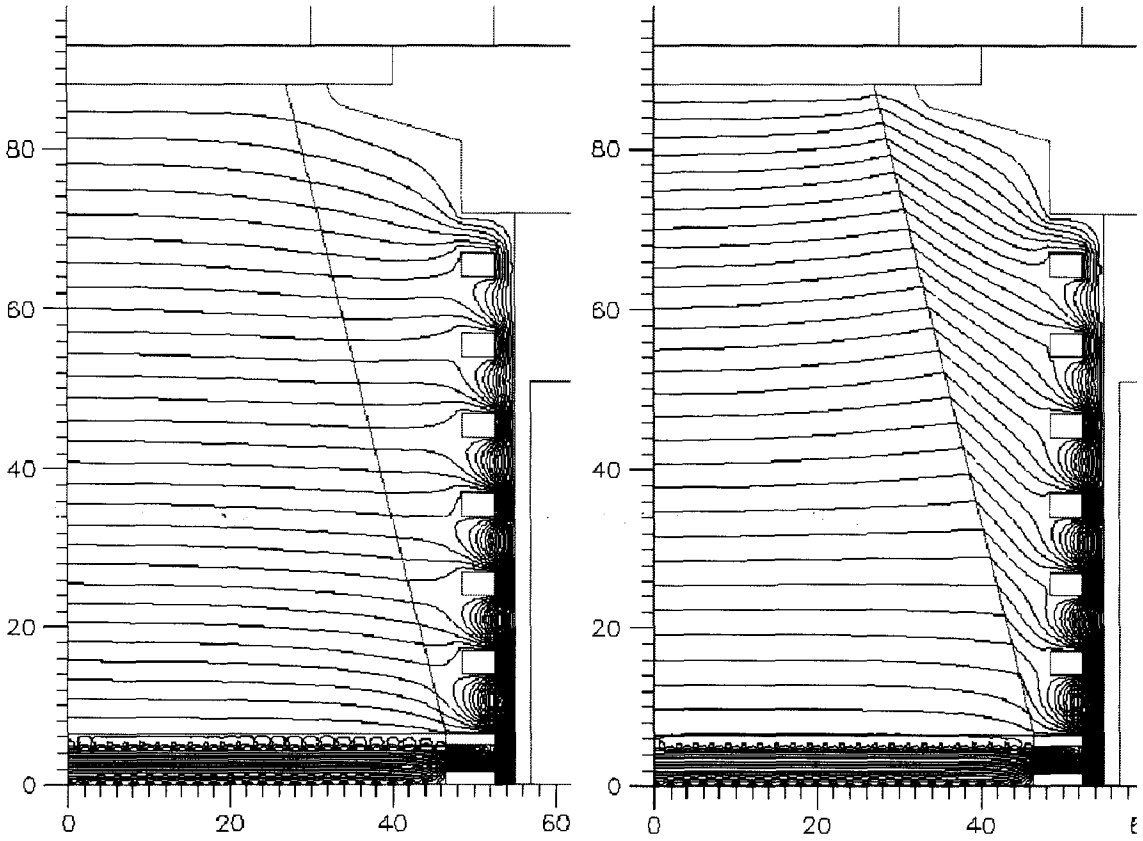

Figure 15 Drift field calculated with simplified model. Left: normal condition. Right: Charged up condition. Electrons will drift downwards. The tilted line is the boundary between the liquid Xe and the Teflon cone.

4.2 Xenon Purification

The most important milestone of the UCLA-Torino dark matter search was the successful test result of the liquid Xe purification (P. Benetti et. al., NIM A329, 1993, 361-364). Based on the ICARUS purification technique, we have developed a special procedure for Xe purification, which yields a purity of less than 0.1 ppb electron negative impurities. This is equivalent to over a few milliseconds of electron lifetime in liquid Xe or a few meters of electron drift distance under normal electric fields (250V/cm).

The lifetime measurement setup is shown in **Figure 16**. Both anode and cathode are shielded by metal grid mesh. Between the two mesh is the region where electron drift. A UV laser shine on the photo-cathode in the chamber produces a large number of electrons. Then the known quantity of charge (measured by the cathode) was injected into the purity test chamber and was collected by anode after it drifted some distance in the chamber. **Figure 17** shows the lifetime result. No charge loss was observed after two hundred-microsecond drifts. The rising edge is the charge injected and the falling edge represents the collected charge. In this particular case, the electrons were drifting under a 10V/cm electric field. With this highly purified liquid Xe, we are in principal able to design a liquid Xe detector with large volume where long electron drift is needed.

Electron drift velocities in liquid Xe under different electric fields and different temperatures (pressure) were measured with the same chamber. The results are shown in **Figure 18**. Notice that the electron drift velocity is independent of the temperature at a drift field around 250V/cm.

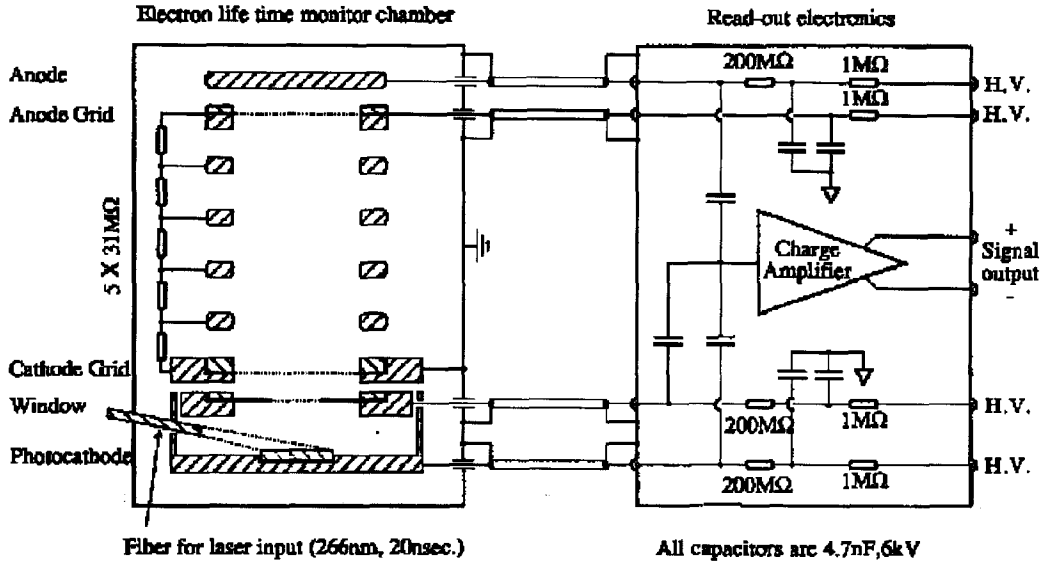

Figure 16 Electron lifetime measurements setup. Purified liquid Xe was filled in the chamber (left box). A laser pulse produces charges. The cathode box are specially made to shift the laser trigger noise. Charge leaving the cathode box and arriving at the anode are both measured with the same amplifier (right).

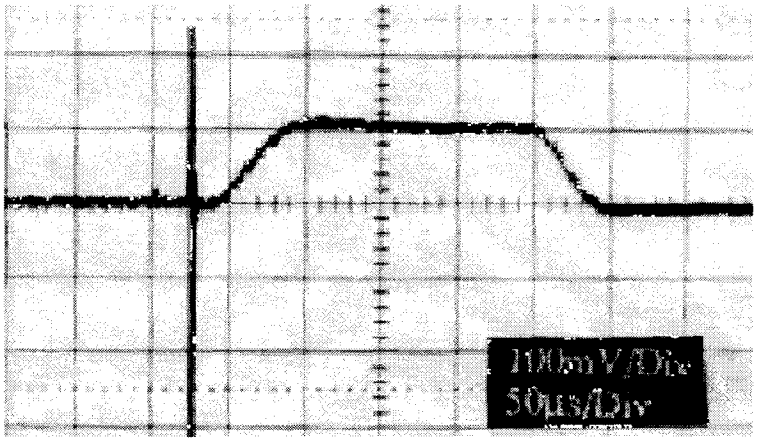

Figure 17 Lifetime measurement results. Electrons drift under an electric field of 10V/cm. The first big spike is the noise from the laser trigger.

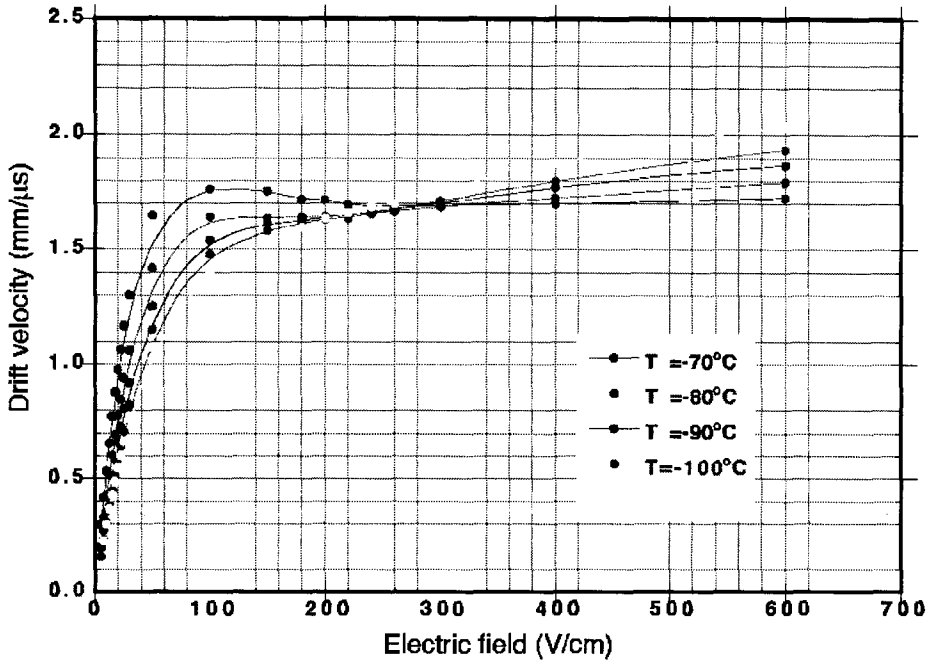

Figure 18 Electron drift velocities under different drift fields E and temperature. Notice that the constant speed at ~ 250V/cm.

4.3 Electroluminescence

When electrons drifting under high electric field in gas xenon, electroluminescence will take place. The number of luminescence photons produced by a single electron under the field of E (kV/cm) at pressure P and drift distant X can be well approximated by the experimental formula:

$$Nph = 70 \quad (\frac{E}{P} - 1.3) \quad X \quad P \tag{3}$$

In the pure liquid case, proportional scintillation was produced with very thin wire (3μm in diameter) at high potential. When electrons drifting very near to the thin wire, due to the very high field near the wire surface, proportional scintillation take place in liquid Xe. The gain in proportional scintillation depends on many factors, such as the surface smoothness of the wire, uniformity of the wire diameter. In the case of 3μm wire, the surface defect due to gold coating can be as big as the wire diameter (seen under electron microscope). While in the case of gas luminescence, the gain N_{ph} depends only on E, P, and X in equation (3). So a very uniform and high gain can be obtained.

Figure 19 shows the results of two-phase in comparison with the single-phase results. Due to the high gain in luminescence, the separation of gamma and recoil are significantly improved. The background rejection power is better than 99.8% in the pure liquid case and is expected to be much better in the two-phase detector.

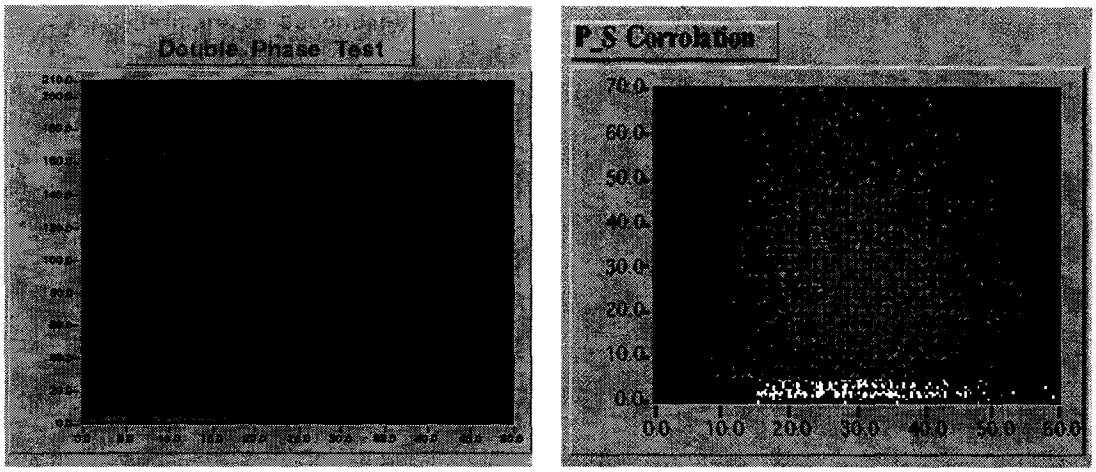

Figure 19 Primary verses Secondary plot in two-phase (top) and single-phase (bottom) Xe.

4.4 Status of ZEPLIN-II project

The central detector is under construction at UCLA dark matter research lab. We have a dedicated lab space for the ZEPLIN-II construction and the main components of the detector have arrived at the lab. as show below. The construction of the central detector will take about four months. Some initial test will be made at UCLA and the system integration is expected to complete during summer 2001 in RAL, UK.

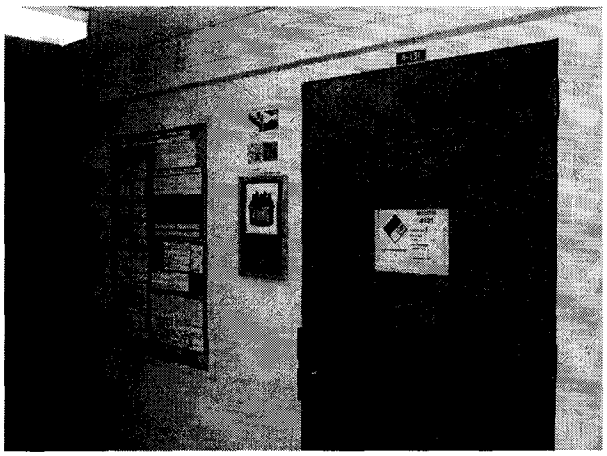

Figure 20 The UCLA Dark Matter lab.

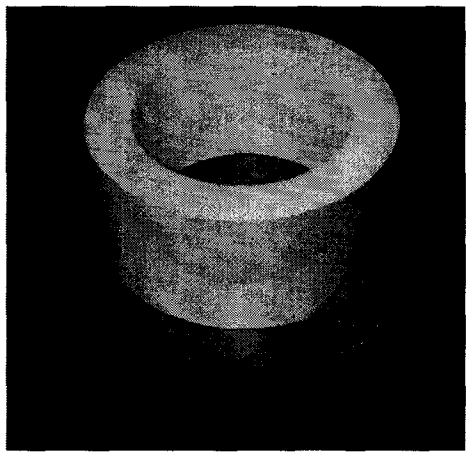

Figure 21 PTFE and copper plates.

The PTFE cone in the ZEPLIN-II design will be made from the PTFE as show above. All field shaping rings, the copper plate holding PMT and, the bottom copper plate will be made out of those copper plate shown above (right).

5 CsI Internal Photocathode for Signal (primary scintillation) Amplification

As stated in §1, Our group's research efforts have been carried out extensively at CERN in collaboration with P. Picchi and the Torino group. Here, we request funding to establish the R&D facility (including a possible transfer of equipment from CERN) to achieve the outlined project objectives at UCLA, considering the significance of having these types of experiment in the US soil. We believe that the proposed research program is crucial as the R&D program for the ultimate liquid Xe dark matter detector possibly at the WIPP site, Carlsbad, New Mexico.

The search for supersymmetric particle WIMPs may require a very sensitive detector capable of reaching 10^{-4} events/kg/day (or less) - this requires very powerful discrimination and a massive detector. Already shown in **Figure 1** a range of models for SUSY WIMPs and the expected rates. Note that very low rates are possible in their models. We also shown in **Figure 1** the expected sensitivities of CDMS II and ZEPLIN II. In order to improve the sensitivity of the liquid Xe detector we need to

(1) increase the mass (say to 500kg).

(2) reduce the energy threshold using the method proposed to be tested here (factor of 10 improvement in sensitivity is possible).

Step (1) can be done based on the ZEPLIN-II structure and our experience with ICARUS experiment. But to reach the sensitivity of 10^{-4} events/kg/day, by step one only, will require a very large detector (few tones of Liquid xenon) which will cost. While a small R&D effort to confirm the signal amplification, will significantly reduce the cost of the future detector. Our R&D results show (discussed below) that it is possible to amplify the signal by a factor of ten, hence the energy threshold will be reduce.

If both of these can be accomplished we may reach the level of sensitivity labeled ZEPLIN IV in Figure 1. Note that this would be very complementary to CDMS II and could help confirm any signal CDMS II may claim in the near future using a totally different technique. For this reason we believe the amplification tests proposed here are very important for the ultimate search for dark matter WIMPs.

5.1 Priciples of CsI luminesence plate

The typical photon wavelength of Xe scintillation is 175 nm. It is hard to collect such hard VUV light with high efficiency. To reduce the photon due to the photon passage through window materials. All PMTs are placed as close as possible to the luminescence region to maximize the light collection efficiency. To get even lower energy threshold, one must develop high Q.E. PMTs or increase the light collection efficiency. The ZEPLIN-II design already maximized the light collection efficiency. If one could amplify the primary signal before it reaches PMT, then the combine with the ZEPLIN-II structure, a perfect detector for dark matter search can be made.

CsI photocathode in liquid Xe has been tested by E. Aprile et al. (NIM A343 1994, 129-134) The typical i-V curves of the CsI internal photo cathode measured in liquid Xe shows a high photocurrent production under a strong electric field (**Figure 22**). Notice that the photo-current in liquid Xe at field above 1.8 kV/cm is greater than that in vacuum. To use CsI as an internal photocathode, we need a very special design to combine the photocathode with the luminescent field.

UCLA group has developed a primary scintillation photon amplification method using a CsI internal photo cathode, luminescence plate in **Figure 23**. It is just a simple thick PCB board with uniform distributed holes (1.4 mm in diametet). In order to coat the CsI on the plate, the surface has to be treated as shown in **Figure 24**. To prevent CsI deposit in the holes, all holes are filled with pins as show in **Figure 26**.

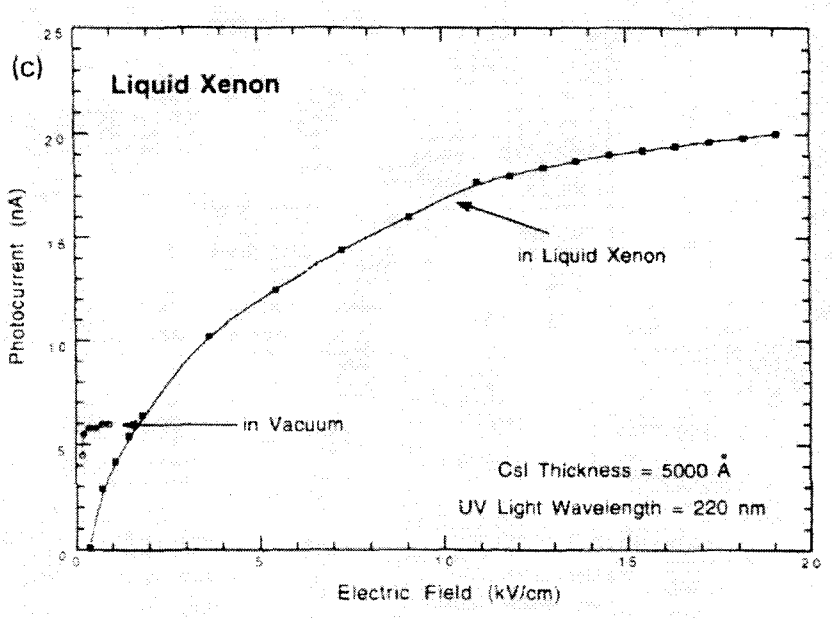

Figure 22 Typical *i-V* curves of the CsI photocathode measured in Liquid Xe and vacuum. (E. Aprile et al. NIM A343 1994, 129-134)

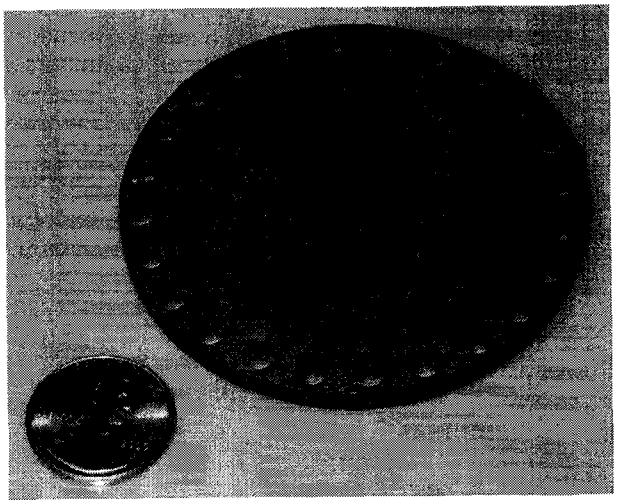

Figure 23 A picture of the CsI luminescence plate with an outer diameter of 66mm (the active CsI part is 50mm); the CsI is exposed in the inner circle (darker area in the picture).

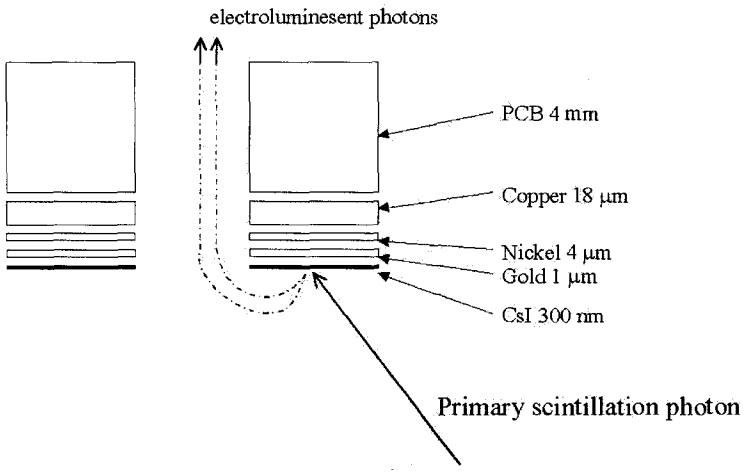

Figure 24 CsI coating on the PCB board.

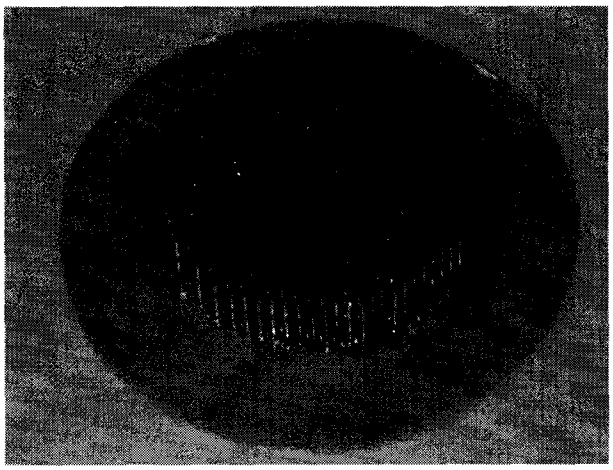

Figure 25 Pin array used to prevent CsI deposite in the holes during coating.

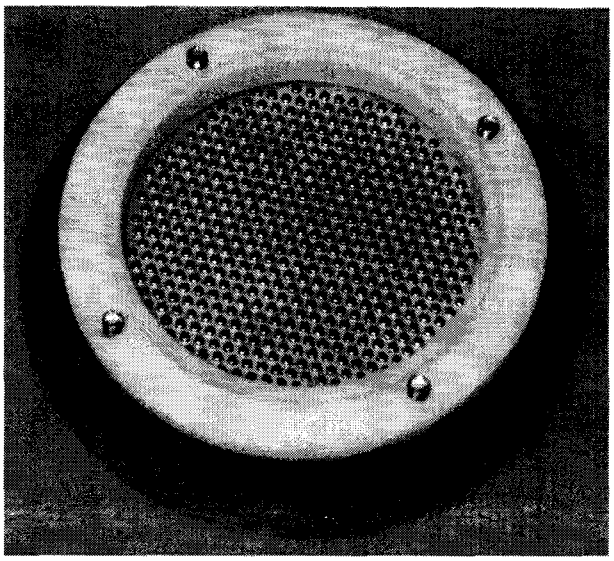

Figure 26 The CsI coating setup. It is then placed in a vacuum deposition chamber for coating at CERN.

The CsI internal photocathode luminescence plate (CPLP) will be place in the chamber with CsI surface face down. And liquid Xe surface will be controlled just above the bottom surface of the CPLP. **Figure 27** (left) shows the simplified 3-D model for finite element analysis (ANSYS installed at CERN). It is a small cell contains one-half hole and two quarter-holes. The calculation stops at the liquid surface. Above the liquid surface, the results is the same except that the dielectric changed from liquid to gas. **Figure 27** (right) shows the result of the calculation in 3-D view with equipotential surfaces. The red lines show the trajectory of electrons coming from the CsI photocathode. The pink lines show the trajectories of electron from ionization in the active region. It is clear that any electron (ionization or photo-electron) below the plate will drift up through the holes. And since the field at the liquid surface is strong enough, all electrons will continue to drift to the gas phase. Again, the field in the gas phase is strong enough for luminescence to take place.

In order to extract electrons from the CsI surface with high efficiency, the field on the surface should be stronger than 1.8 kV/cm as suggested from **Figure 22**. With careful arrangement this can be achieved and the calculated results from ANSYS is shown in **Figure 28**. This confirms that the minimum field at the CsI surface is greater than 1.8kV/cm.

The working process is as the following. The primary scintillation photons from event in the active region will hit the CsI surface and produce photo-electrons. Then the photo-electrons will be extracted by the strong field at the surface, and will continue to drift along the trajectories shown in **Figure 27**. So the CsI internal photocathode luminescent plate converts the primary scintillation photon and then amplifies it through electrolumienscence process.

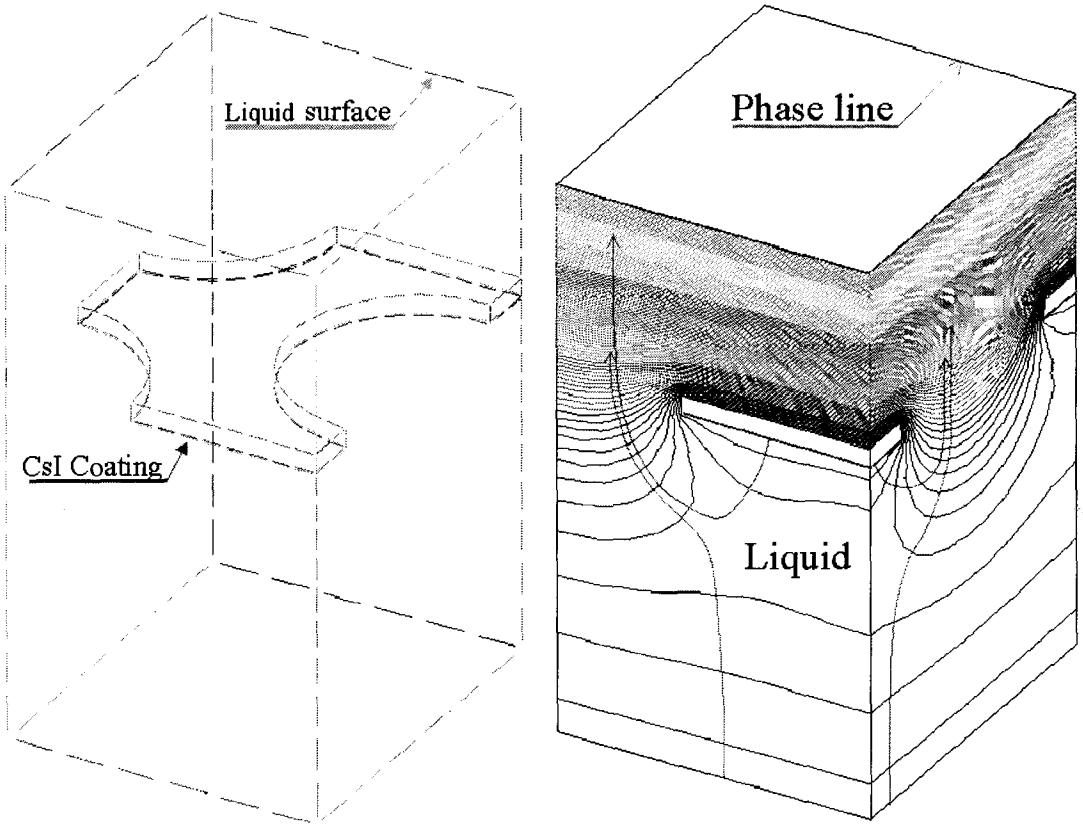

Figure 27 The drift trajectory of photoelectrons (from bottom surface) and ionization electrons.

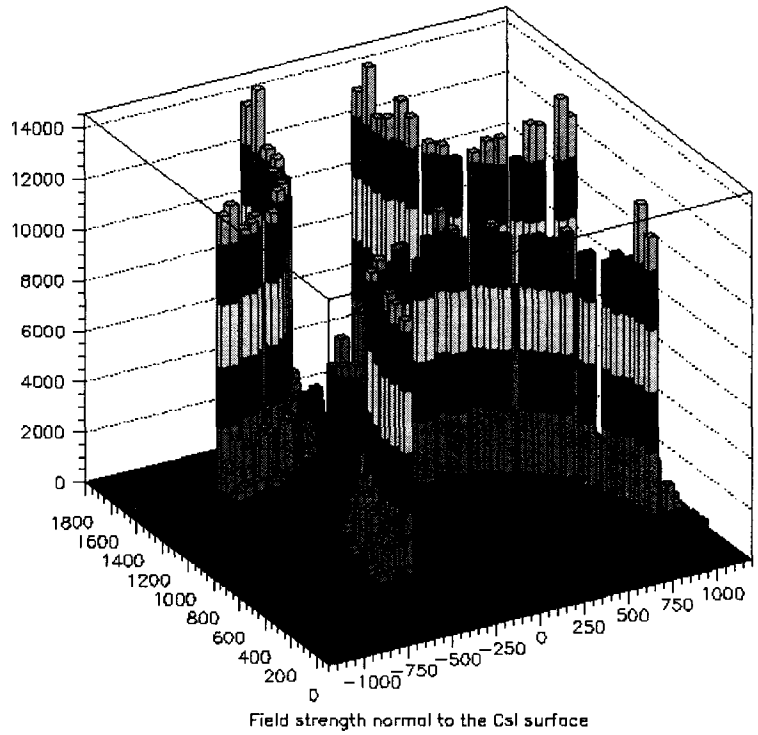

Figure 28 Electric field at the surface of CsI. Horizontal axis are the location on the plate. The vertical axis is the field normal to the surface in V/cm.

5.2 Initial test results

A quick test was make at CERN with gas only. This is a test without the need for cryogenic and purification system. The simple setup is shown in **Figure 29**. Over 2.5kV is applied between the luminescent plate. No special UV lamp was used. We only trigger on the background signals in the chamber filled with gas Xe. Two typical signals are shown in **Figure 30**. Notice that there is no drift field below the plate in this test condition to avoid ionization electron drift up which may be mixed with those photo-electrons.

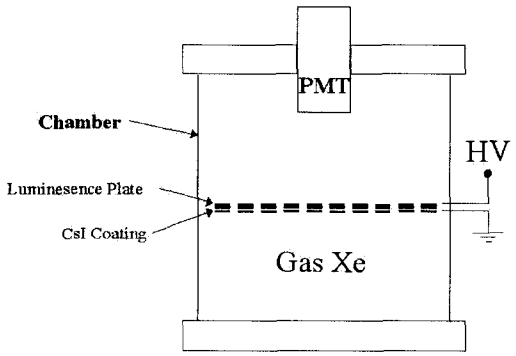

Figure 29 A simple diagram of the experimental setup of the CsI internal photo cathode for one phase Xe (left) and two-phase Xe (right).

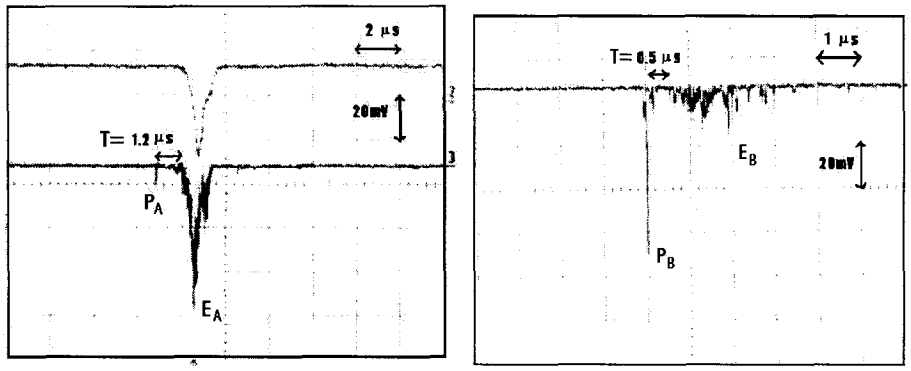

Figure 30 Typical signals from the experimental setup with CsI internal photo cathode in the one phase Xe test chamber. Normal amplification signal (left) and when the gamma-Xe nucleus interaction occurs near the plate (right).

The typical drift time from CsI surface to the holes is about 1.2 μs as shown in the figure. The ratio secondary signal to primary signal (S/P) is about 20 (**Figure 30** left). Assuming 0.2 as the quantum efficiency of PMT, The estimated gain (number of photons per electron) is about 200 which is in a good agreement with N_{ph} (number of electroluminescent photons) from eq. (3) in §4.3. **Figure 30** (right) shows a large gamma-Xe nucleus interaction occurs near the luminescence plate. Since electric field is non-zero near the plate, ionization electron produces electroluminescent photons immediately after the event.

The overall gain when solid angle and other factor are considered is about 10. This is a very encouraging results. A systematic study in two-phase should be carried out to confirm the gain. liquid and gas. This simple and effective solution could be used in the current ZEPLIN-II upgrade in the future and or, applied to the future large scale dark matter detector. A future large scale detector based on ZEPLIN-II and the CsI internal photocathode could be realized as shown in **Figure 31**. It is only 500kg and already sensitive to most SUSY region as shown in **Figure 1**.

5.3 Proposed test of the CsI luminescence plate at UCLA

The simple experimental setup at CERN (**Figure 29**) uses only gas phase Xe for the signal amplification. It must be significantly improved in order to do the two-phase test. To fully utilize the UCLA teams experience, student trainning in the US and foreseen a large scale development of the future dark mater experiment in the US. We propose to carry out the test in UCLA.

The test system at UCLA is shown in **Figure 32**. xxx oe A two-phase test In parallel with ZEPLIN-II two-phase Xe design, the same test for signal amplification is needed with two-phase Xe test chamber (**Fig 25bxxxxx**). Although the proposed test chamber construction at UCLA is similar to the test chamber built at CERN for gas phase only, the cost of construction could be initially higher because we have less support at this moment. We request funding for the facility to build the initial test chamber, which, once completed, will reduce the cost of future R&D work for the ultimate dark matter detector with 500kg liquid Xe target.

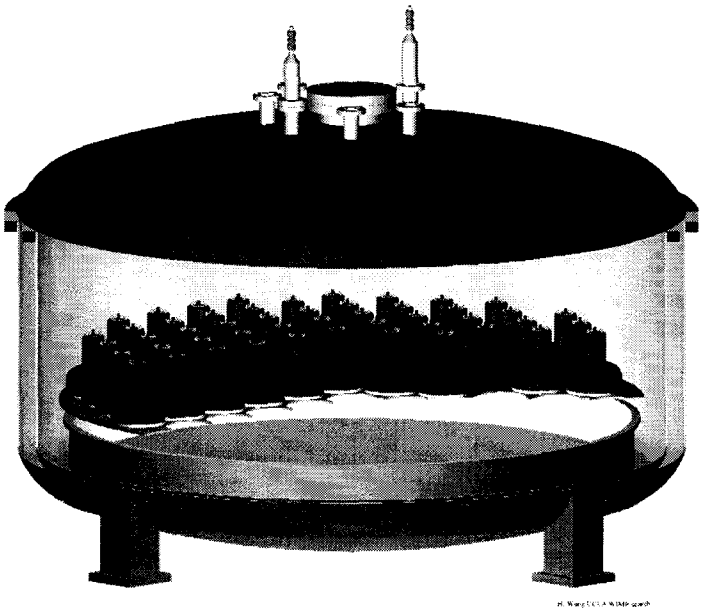

Figure 31 The conceptual drawing of ZEPLIN IV detector (500kg liquid Xe target) based on the ZEPLIN-II design and the expected CsI internal photocathode results. (Electronics and field shaping rings are not shown).

5.4 Proposed R&D program for primary scintillation photon signal amplification

The proposed test cell is show in **Figure 32**. The actual test cell (left) will be placed in a vacuum thermal insulation chamber. All gas, cooling and signal feed-through will be placed on the vacuum chamber's top flange (not show). **Figure 33** conceptual drawing of the system set up.

The liquid cell is about 250 cc in volume, (about 70 mm diameter cylinder of 13 mm thick) (the liquid cost $975 in a commercial bottle at 99.995 purity, will be purified again be fore the test). A Magnesium Fluorine window is used to seal the chamber and to let the 175 nm UV light go through. A 2-in PMT (with MgF window) placed on top of the window in the vacuum reads the signal. Two HV feed-through (at back, not shown) will be used to set the potential on both side of the CsI plate. The maximum voltage needed is less than 5000V (between the CsI plate).

The cooling system (cooling contact not shown) is a 'Standard CRYOTIGER' from IGG APD Cryogenics Inc. has 27 watts cooling power and cools down as low as 145K using PT-30 gas mixture ($7,360). This cryogenics system can be a very good lab system for future R&D. By changing the gas mixture, it can cool down as low as 94K using PT-14.

Vacuum will be made by an all in one system, 'Tribodyn' from DANIELSON Vacuum products, Inc. It is a completely oil free system able to pump a 30 Liter volume down to 10^{-9} torr ($10,750). The test system has two separate vacuum cells, the test cell and the vacuum thermal insulation. The two cells can be pumped by the same vacuum pump and when filling liquid Xe, we simply switch the pumping to the insulation cell. Of cause this will require equal care on the cleaning both inside and outside of the test to avoid contamination to the Xe cell.

We propose to buy a 100 MHz digital oscilloscope, TDS-3012 by Tektronix ($2,995 + GPIB interface $995), to be used for both system debug and data acquisition. The sampling rate on each channel (two channels) is 1.25 GS/s (or 0.8 ns /sample). The fastest component from the Xe scintillation is above 20 ns for unshaped signal. With maximum record length of 10k points each channel, the scope can sample 8 μs in one shot. We should be able to sample 13 mm drift if the

drift field are set at 250 v/cm (see **Figure 18**). For systematic studies of the CsI amplification, we will store all data via GPIB interface to a PC for analysis.

This test will determine the photo-electron extraction efficiency and luminescence gain at the gas part in the holes of the luminescence plate. Since all the principles are already tested in different setup by other authors for different purpose, we believe that the objective of this proposal will have positive results.

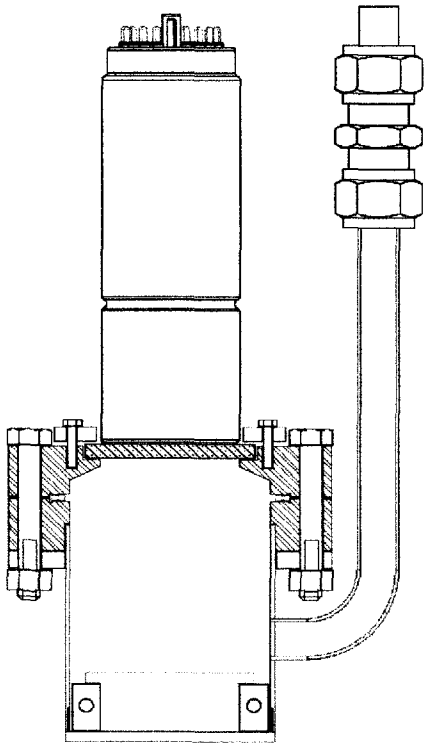

Figure 32 The proposed CsI internal photocathode test system with two-phase Xe at UCLA. (left) the actual test cell. (right) Vacuum thermal insulation chamber.

Figure 33 Conceptual drawing of the system setup.

6 Conclusion

Figure 33 system setup

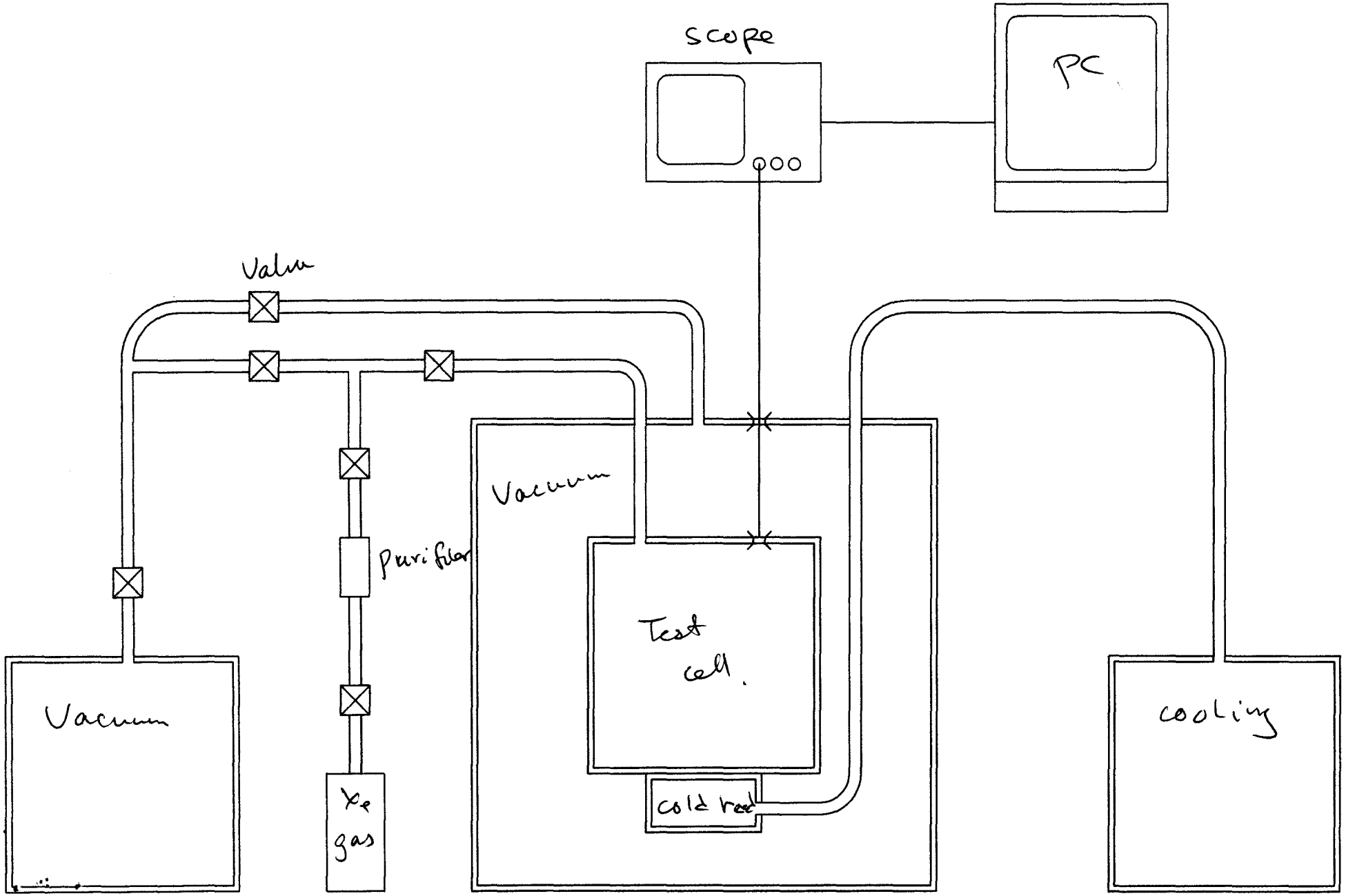

7 Budget & Commentary

8 Current and Pending Support Statement

9 Biographical Sketches